Satellite-based Study of Interannual Variation of Abundance and Seasonal Transport of Giant jellyfish, *Nemopilema nomurai*, in the Yellow Sea and East China Sea

(黄海と東シナ海での大型クラゲ　*Nemonilema nomurai*　の現存量経年変動と季節的輸送に関する衛星による研究)

By

Xu, Yongjiu

（許　永久）

A dissertation for the degree of Doctor of Science

Department of Earth and Environmental Sciences,

Graduate School of Environmental Studies, Nagoya University

（名古屋大学大学院環境学研究科地球環境科学専攻学位論文　博士（理学））

2014

Abstract

Jellyfish of species Scyphozoa and Hydrozoa have risen in numbers extensively in the world oceans. The causes and consequences of jellyfish abundance and distribution are great concerns to the human beings, since human enterprises (tourism, fishing, aquaculture and power production) were interfered with the jellyfish. Due to fragile gelatinous body and difficulties of conventional sampling, quantitative records and environmental change data on jellyfish abundance and distribution are rare. Satellite data with high temporal and spatial resolution would be useful for detecting environmental variables related to jellyfish, thus, acting as good indicators of variation of abundance and spatial distribution. Outbreaks of giant jellyfish *Nemopilema nomurai* have become one of the biggest problems for marine ecosystem in the Yellow Sea (YS), East China Sea (ECS) and the Sea of Japan from 2002 to 2009. This study is to explain the interannual variation of the giant jellyfish outbreaks and the transport of the jellyfish by satellite derived environmental indicators in the YS and ECS.

In Chapter 2, the driving factors in *N. nomurai* outbreaks and the recent absence were studied. Three hypotheses (temperature, eutrophication, and match–mismatch) were examined for young jellyfish (ephyrae) by using satellite sea surface temperature (SST) and chlorophyll a (Chl-*a*) during spring and summer. Warm temperatures have been suggested to increase polyp strobilation and ephyral growth in *N. nomurai*; eutrophication may increase the phytoplankton biomass, which probably further enhance zooplankton production to supply more food to jellyfish; match condition between ephyral stage and phytoplankton bloom may also provide high food availability for ephyrae. These environmental conditions were thus suggested to favor *N. nomurai* outbreaks. Differences in environmental variables (SST, Chl-*a*) among pre-jellyfish years (PJY: 1998–2001), jellyfish years (JY: 2002–2007, 2009), and non-jellyfish years (NJY: 2008, 2010) were assessed. Firstly, temperature hypothesis was examined by comparing the SST difference between PJY, JY and NJY. The SST during late spring and early summer increased significantly from 1985 to 2007, indicating that high SST is beneficial to the long-term increases in jellyfish outbreaks. SST was significantly lower in NJY than in JY, suggesting that low SST might reduce the proliferation of *N. nomurai*. Then, the eutrophication hypothesis was investigated through analyzing long-term variation of Chl-*a*. Both Chl-*a* during non-blooming periods and the peak increased significantly from 1998 to 2010 in most of the YS and ECS, indicating that eutrophication is beneficial to the increases in jellyfish outbreaks. Furthermore, we examined the match-mismatch hypothesis. We focused on the timing of SST reaching

15°C, a critical temperature enabling polyps to induce strobilation and allowing released ephyra to grow. We analyzed the relationship with the timing of interannual variability of SST and the timing of phytoplankton blooms. Timing of phytoplankton blooms varied interannually and spatially, and their match and mismatch to the timing of SST reaching 15°C was not corresponded to the increases in *N. nomurai* outbreaks and the recent absence. Further, a conceptual model was developed to explain the jellyfish outbreak and absence based on the three hypotheses.

In Chapter 3, the spatial distribution of the giant jellyfish and its relation to water masses and circulation were investigated by ship observation, in combination with satellite data and particle tracking experiments. The temperature and salinity of observed stations were examined by hierarchical clustering; the results showed that there are six main and two mixed water masses in the surface layer. The high abundances of giant jellyfish were observed in southern YS water, waters between Changjiang diluted water (CDW) and Changjiang upwelling water, and mixed waters between CDW and Kuroshio warm water, while few were observed in other water masses. Then, satellite data were used to characterize the seasonal variation of the water mass. The results indicated that as the winter monsoon weakens, water mass with warmer SST (>15^{o}C) in Jiangsu coast in May was advected to north and northeastward until July. The southerly wind was probably important factor to induce this northeastward circulation. This indicated that the wind contributed to the advection of young medusa from the coast to northward offshore from May. Moreover, transport of jellyfish from the potential source was reasonably simulated by backward trajectory model, and further verified by forward trajectory model and an independent observation data. The water mass with jellyfish was traced back to the northern Changjiang mouth through Jiangsu coast in late April or early May. While, water mass without jellyfish were stayed in the offshore of the YS, or traced back Changjiang mouth inlet and Taiwan Strait. These findings indicated that the high abundance of *N. nomurai* observed in the YS and ECS in July came from the north of the Changjiang mouth to northern Jiangsu coast in May when ephyrae were probably liberated from polyps there with SST increased from below 15^{o}C to higher.

This study is the first to show the feasibility and advantages of using satellite derived environmental factors to explain the interannual variation and seasonal transport of the giant jellyfish *N. nomurai* in YS and ECS. The satellite-based study conducted here can not only be applicable for *N. nomurai* in the YS and ECS, but also for other pelagic species (e.g. fish larvae, plankton) in other areas, thus it has immense significance in research of marine ecosystem.

Table of Contents

List of Tables

List of Figures

Abbreviations

AVHRR	Advanced Very High Resolution Radiometer
BITT	Backward-in-time trajectory
BS	Bohai Sea
CDW	Changjiang Diluted Water
Chl-*a*	Chlorophyll *a* (mg m^{-3})
CJE	Changjiang Estuary
CPUE	Catch per unit effort
CSDP	Coast of the Shangdong Peninsula
CSYS	Chinese coast of the southern Yellow Sea
CTD	Conductivity-temperature-depth
CUW	Changjiang Mouth Upwelling Water
ECS	East China Sea
FIIT	Forward-in-time trajectory
JCOPE2	Japan Coastal Ocean Predictability Experiment 2
JRA-25	Japanese 25-year Reanalysis
JY	Jellyfish outbreak year
KOSC	Korea Ocean Satellite Center
KSYS	Korean coast of the southern Yellow Sea
KWC	Kuroshio Warm Current
MODIS	Moderate Resolution Imaging Spectroradiometer
MNYS	Middle of the northern Yellow Sea
MSYS	Middle of the southern Yellow Sea

NJY	Non-jellyfish outbreak year
nLw(555)	Normalized water-leaving radiance value of 555 nm
NOAA	National Oceanic and Atmospheric Administration
NYSW	North Yellow Sea Water
PJY	Pre-jellyfish outbreak year
Rrs	Remote sensing reflectance
S	Salinity
SeaWiFS	Sea-viewing Wide Field-of-view Sensor
SST	Sea-surface temperature
SYSW	South Yellow Sea Water
T	Temperature
Tsst15	Timing of SST reaching 15^{o}C
TWC	Taiwan Warm Current
YOC	Yellow Sea Large Marine Ecosystem Ocean Color Work Group
YS	Yellow Sea
YSCC	Yellow Sea Coastal Current
YSWC	Yellow Sea Warm Current

Chapter 1: General Introduction

1.1. Background of the *Nemopilema nomurai* in the Yellow Sea and East China Sea

The giant jellyfish, *Nemopilema nomurai*, is the species of the class Scyphozoa in the phylum Cnidaria. With bell diameter as large as ca. 2 m and wet weight as heavy as 200 kg (Kawahara et al., 2006; Omori & Kitamura 2004), the giant jellyfish was noted for its hazardous effect, for example, reduced fishery production, stinging of swimmers and even causing one boat to capsize (Purcell et al., 2007; Dong et al., 2010; Uye 2011). Giant jellyfish is distributed mainly in the East Asian marginal seas, including the Bohai Sea (BS), the Yellow Sea (YS), the East China Sea (ECS), and the Sea of Japan (Kawahara et al., 2006; Uye 2008). The medusae were transported to the Sea of Japan by Tsushima current from the main habitat, i.e. the BS, YS and ECS (Uye 2008), which has been undergoing long-term modifications due to human activities such as the use of chemical fertilizers, dam construction, and land modification (Gao and Song, 2005; Kim et al., 2009; Li et al., 2007). Massive outbreaks of *N. nomurai* have historically been extremely rare, occurring approximately once every 40 years, in 1920, 1958, and 1995 (Yasuda, 2004; Uye 2011). However, since 2002, outbreaks of *N. nomurai* have become more frequent and more extensive across YECS areas, occurring every year except 2008, 2010, and 2011 (Fisheries Research Agency, Japan: http://jsnfri.fra.affrc.go.jp/Kurage/kurage_top.html; accessed 18 March 2012). During the jellyfish outbreak years, up to 1500 medusae have been caught in a set-net in a single day in Japanese coast (Kawahara et al., 2006), however, it was not abundant, with one or two medusa per week during the non-outbreak years (Kawahara and Dawson 2007). The extensive and consecutive of the giant jellyfish outbreaks in Yellow Sea (YS), East China Sea (ECS) and the Sea of Japan caused serious damage to the marine

ecosystem and its dependent economy of northeastern Asian countries in recent decades. The decline of fisheries in the YS and ECS Chinese waters were associated with the increase of giant jellyfish blooms, with the catch per unit effort (CPUE) of commercial fisheries decreasing about 20%, and maximum biomass of giant jellyfish reaching 15000 kg/ha (Ding and Cheng, 2007; Dong et al., 2010). The nuisance to fisheries created by *N. nomurai* has been reported from at least 17 prefectures of Japan (www.jsnf.affrc.go.jp/) (Kawahara et al., 2006). The causes of the jellyfish outbreaks were suggested to be attributed to the anthropogenic and environmental changes, which was evident in the BS, YS and ECS coastal waters. Origins as well as jellyfish distribution are also great concerns to the scientific community, since these knowledge provide accurate early-warning of the potential risk of fisheries activities, power plants and bathing beaches, which was usually occurred in these waters (Dong et al., 2010).

1.2. Life cycles of *N.nomurai* in the Yellow Sea and East China Sea

Like most of the Scyphozoa, *N. nomurai* has a complex life cycle, with alternate sexual (pelagic) and asexual (benthic) stages. We focused on the life cycle, starting from formation of polyps, as stages after polyp played more important roles in outbreak of jellyfish. The planulae, which was developed 1 day after the fertilization of eggs, underwent morphogenesis after settlement in the suitable substrate (including plastic floatings, kelp or seaweeds and man–made structures such as oil platforms and harbour walls) to form polyps (Kawahara et al., 2013), although Kawahara et al. (2006) reported the morphogenesis occurred in the air-water interface in the laboratory experiment. The goblet-shaped scyphistomae is like a single fully functioning organism system. The scyphistoma firstly moved to the new attachment site, leaving a podocyst behind at the former position. Then, the podocyst excyst to forma a new scyphistoma when the

condition (temperature, salinity, food etc.) was favorable, asexual reproduction will continue until polyp segment through the strobilation process (Kawahara et al., 2006, 2013). With the temperature increased from below 15^{o}C to higher, scyphistomae elongated and segmented, and formed as strobila. The segments of fully developed strobila separate one by one to become free swimming ephyrae, which develop to the adult stage (the medusa) (Kawahara et al., 2006).

1.3. Previous studies about *N.nomurai* in the Yellow Sea and East China Sea

The seasonal increase of the jellyfish abundance always occurred between June and September (Yoon et al., 2008; Zhang et al., 2012), this seasonal peak is also a characteristic of marine environments, however, interannual variability of jellyfish abundance is also obvious in these waters as described above. The abundance of jellyfish was suggested to be reflected by the success of excysting during the podocyst stage and the production of ephyrae in the polyp stage (Uye, 2008; Purcell et al., 2009; Kawahara et al., 2013). Previous studies focusing on the podocyst stage suggested a switch mechanism between outbreak and non-outbreak according to the laboratory experiment. Polyps are much more resistant to environmental fluctuations, and in poor conditions polyps may encyst–a state similar to hibernation-at least 6 years. However, under good condition, massively accumulated podocysts would excyst extensively to build up a large polyp population size (Kawahara et al., 2013), forming a potential outbreak year. The factors inducing the jellyfish outbreak are still unclear, exposure to lowering salinity, recovery from hypoxia as well as burial in the mud were suggested to be probable factors to induce podocyst to excyst (Kawahara et al., 2013). For the stage after polyp, especially for the survival of ephyral stage, temperature, eutrophication

were suggested to be important factors (Kawahara et al., 2006; Uye, 2008; Purcell, 2012). By laboratory experiments, warm temperatures have been confirmed to increase polyp strobilation and ephyral growth in *N.nomurai* (Kawahara et al., 2006; Purcell et al., 2009). Eutrophication would enhance secondary primary production (zooplankton production), thus, could supply more food to jellyfish (Uye 2008; Purcell 2012).

The spatial distribution and transport of giant jellyfish was another important topic in the scientific community. Zhang et al., (2012), found that the giant jellyfish was confined in the water mass of YS and northern ECS, with concentrated jellyfish in the salinity range of 32-33, while, few were observed in the water mass of southern ECS, according to a large-scale bottom trawl survey. With visual observation in the south and southwest of Jeju island, Yoon et al. (2008) observed high abundance of jellyfish in the west of Jeju, and few in the east and south of Jeju. Based on a numerical model, Moon et al. (2010) found that the jellyfish particles in Changjiang mouth were transported to Tsushima strait and were advected to the Sea of Japan later time. However, most of the jellyfish particles released in northern Jiangsu coast were confined in the YS, not passing the Tsushima strait. The water mass and circulations were suggested to play important roles in the distribution and transport of jellyfish from the potential sources (Kawahara et al., 2006; Yoon et al., 2008). Yoon et al. (2008) surmised that ephyrae were transported southward from YS coast to the area near Changjiang mouth in early spring, and then were drifted with spreading CDW driven by southerly wind from May. Kawahara et al. (2006) also highlighted this drift pattern and further estimated that strobilation and ephyral liberation may take place in spring and early summer when water temperature increased from 10 to 20 ^{o}C in the YS and ECS coast. Meanwhile, some studies of green algae suggested the northward drift since late spring. Lee et al.

(2011) suggested the green algae patch were drifted to the north or northeastward to the Qingdao and its offshore by current and wind since April. The interannual variation of green algae path was highly correlated with wind magnitude and direction. Huo et al. (2013) suggested that the green algae starts to appear Jiangsu coast in April, and drifts to the offshore caused by the tidal current, and then is transported toward north to the YS and its offshore.

Satellite-detected sea-surface temperatures (SST) and ocean color (Chl-*a*) have been used to characterize physical and ecosystem features, respectively, in the YECS (Hickox 2000; Yamaguchi et al., 2012, 2013). These satellite data are useful to monitor physical features, eutrophication and harmful algal blooms, which was directly or indirectly related with variation of jellyfish abundance and distribution (Ahn and Shanmugam 2006; Gremillet et al., 2008; Yamaguchi et al., 2013).

1.4. Objective of this study

Due to the large spatial scales of giant jellyfish distributions, traditional oceanographic observations would be difficult to apply in this kind of study. Satellite data are expected to be useful to detect temporal and spatial variation and magnitude of environments related to jellyfish outbreaks. Hence, the objectives of the study are to (1) test the three hypotheses (temperature, eutrophication, and match–mismatch) using satellite SST and Chl-*a* data, in order to determine the driving factors behind the long-term outbreaks in *N. nomurai* and recent absence, (2) investigate jellyfish distribution and its relation with water mass and examine and verify the transport of jellyfish from potential source through ship observation, satellite data and particle tracking experiment. The ship observed jellyfish distribution was used for the particle

tracking experiment, the accuracy was evaluated by comparison between ship observed and modeled environmental variables. The satellite data were used to verify and support the modeled results.

1.5. Structure of this Dissertation

This thesis is divided into 5 chapters. The 1st chapter provides general introduction in view of background and life cycle of *N. nomurai*, and objectives of this study. The 2nd chapter tests the three hypotheses (temperature, eutrophication, and match–mismatch) using satellite SST and Chl-*a* data. The 3rd chapter describes the jellyfish distribution and its relation with water mass based on ship observed data, and then examines the transport of observed water mass with or without jellyfish through particle tracking experiment and satellite data, and finally, verifies the transport of jellyfish from the source by comparison with independent ferry observation. The 4th chapter discussed the findings of this study in general. The 5th chapter provides general conclusions from the previous chapters.

Chapter 2: Relationships of interannual variability in SST and phytoplankton blooms with giant jellyfish (*Nemopilema nomurai*) outbreaks in the Yellow Sea and East China Sea

2.1. Introduction

The Yellow Sea and East China Sea (hereafter YECS), the largest continental marginal seas in the western North Pacific Ocean (Jiao et al., 2007), are surrounded by China, Korea, and Japan (Fig. 2.1). They are connected to the Pacific Ocean, the South China Sea, and the Sea of Japan by the strait between Taiwan and the Ryukyu Islands, the Taiwan Strait, and the Tsushima Strait, respectively. YECS areas are highly dynamic with a variety of distinguishable water masses. The area is characterized by a wide continental shelf (<200 m depth) and extremely dynamic seasonal river runoffs (Zhang et al., 2007; Siswanto et al., 2008; Kim et al., 2009a). The freshwater runoffs, especially from the Changjiang River, and oceanic currents, such as the Kuroshio and Taiwan warm currents, induce major circulation patterns in the YECS. The Changjiang estuary (CJE) and its adjacent YECS waters are highly productive and resource-rich (Beardsley 1985). However, this ecosystem is also sensitive to variations in runoff from the Changjiang River, which has been undergoing long-term modifications due to human activities such as the use of chemical fertilizers, dam construction, and land modification (Gao and Song 2005; Li et al., 2007; Kim et al., 2009b). Dissolved inorganic nitrogen levels have been increasing in the YECS since the 1980s, as influenced by the Changjiang River Discharge (Siswanto et al. 2008), terrigenous nitrogen fertilizer utilization (Wang 2006), and coastal aquaculture (Hu et al. 2010). Eutrophication due to increased nutrients has generated more frequent algal blooms in Chinese coastal waters since the 1990s (Tang et al. 2006).

Nemopilema nomurai, one of the largest jellyfish species in the world, is distributed mainly in the East Asian marginal seas, including the Bohai Sea (BS), the Yellow Sea, the East China Sea, and the Sea of Japan (Kawahara et al., 2006; Uye 2008). Massive outbreaks of *N. nomurai* have historically been extremely rare, occurring approximately once every 40 years, in 1920, 1958, and 1995 (Yasuda 2004; Uye 2011). However, since 2002, outbreaks of *N. nomurai* have become more frequent and more extensive across YECS areas, occurring every year except 2008, 2010, and 2011 (Fisheries Research Agency, Japan: http://jsnfri.fra.affrc.go.jp/Kurage/kurage_top.html; accessed 18 March 2012). Previous studies have suggested that anthropogenic environmental changes such as eutrophication, habitat modification, overfishing, and global warming are responsible for these recent outbreaks (Purcell et al., 2007; Uye 2008; Uye 2011). *N. nomurai* has a complex life cycle, with alternate sexual and asexual stages. The abundance of jellyfish reflects the success of excysting during the podocyst stage and the production of ephyrae in the polyp stage (Purcell et al., 2009). Judging from the occurrence of young medusae, Kawahara et al. (2006) speculated that the strobilation of polyps occurs in late spring to early summer in the YECS. During a recent survey, ephyrae were found for the first time in the northwestern East China Sea, and detachment from polyps was estimated to have occurred in early May near the mouth of the Changjiang River and along the coast of Jiangsu Province (Toyokawa et al. 2012).

To determine the driving factors behind the recent outbreaks in *N.nomurai*, we examined three hypotheses (temperature, eutrophication, and match–mismatch) during the ephyral stage in YECS. Temperature increases raise the physiological rates of both phytoplankton and the herbivorous zooplankton that feed on them (Sommer and

Lengfellner 2008). With more jellyfish appearing in warmer years, temperature-related effects could become evident in polyp strobilation and ephyral growth (Richardson et al., 2009). In laboratory experiments, warm temperatures have been confirmed to increase polyp strobilation and ephyral growth in *N. nomurai* (Kawahara et al., 2006; Purcell et al., 2009). A temperature of 15ºC is critical, allowing released ephyrae to grow (S. Uye, personal communication) and producing the highest cumulative strobilation rate for *N. nomurai* (Kawahara et al. 2013).

Eutrophication due to increased nutrient input may increase the phytoplankton biomass, which may further enhance zooplankton production to supply more food to jellyfish (Uye 2008; Purcell 2012). Additionally, eutrophication could cause more frequent flagellate-phytoplankton blooms. Changes in the food web may reduce the size of the zooplankton community, leading to more favorable conditions for jellyfish than for fish (Purcell et al. 2007; Richardson et al. 2009; Purcell 2012). Moreover, eutrophication with enhanced organic matter production may contribute to the frequent occurrence and greater intensity of hypoxia/anoxia in coastal waters (Chai et al. 2006), which would probably benefit jellyfish rather than fish (Purcell 2012).

The match–mismatch hypothesis predicts that the growth and survival of the larvae of marine predators depends on a temporal match with prey availability (Cushing 1990; Durant et al. 2005). A number of studies have indicated that top predators (e.g., jellyfish, fish) are indirectly controlled by primary production via bottom-up processes, and this hypothesis seems to be applicable for a wide range of marine predators (Frank et al. 2007; Gremillet et al. 2008).

Satellite-detected sea-surface temperatures (SST) and ocean color (Chl-*a*) have been used to characterize physical and ecosystem features, respectively, in the YECS (Hickox 2000; Yamaguchi et al. 2012, 2013). These satellite monitoring data are useful to monitor eutrophication and harmful algal blooms (Ahn and Shanmugam 2006; Yamaguchi et al. 2013). Due to the large spatial scales of giant jellyfish distributions, traditional oceanographic observations would be difficult to apply in this kind of study; instead, satellite images of SST and Chl-*a* are useful for detecting environmental variables related to jellyfish outbreaks. The Chl-*a* is also expected to serve as an indicator of zooplankton abundance (i.e., food for jellyfish) (Gremillet et al. 2008).

The objective of this study was to test the three hypotheses (temperature, eutrophication, and match–mismatch) using satellite SST and Chl-*a* data. Interannual variability in spring and early summer (March–June) SST were investigated, and interannual variability in the timing and magnitude of phytoplankton blooms were compared with the timing of SST reaching 15°C (hereafter Tsst15). In the following sections, we described the environmental characteristics during pre-jellyfish years (PJY, 1998–2001), jellyfish years (JY, 2002–2007, 2009), and non-jellyfish years (NJY, 2008, 2010), and discuss the factors controlling the outbreak of giant jellyfish.

2.2. Materials and methods

2.2.1. SST dataset

The SST data used in the present study were 8-day averaged (hereafter 8-day weekly) and monthly nighttime, 4-km resolution data from Pathfinder version 5 AVHRR/NOAA (Advanced Very High Resolution Radiometer) for 1998–2002 and

from MODIS/AUQA (Moderate Resolution Imaging Spectroradiometer) Level 3 for 2003–2010 (Table 2.1). The AVHRR and MODIS data were screened for quality control. Only pixels with quality levels of 4–7 were used (http://www.nodc.noaa.gov/SatelliteData/pathfinder4km/userguide.html) as well as level 0 data (http://oceancolor.gsfc.nasa.gov/DOCS/modis_sst/). We used the combined 8-day weekly/monthly datasets (1998–2010) for further study, as the accuracy of the MODIS SST data was consistent with the AVHRR Pathfinder SST fields (Minnett et al. 2002).

2.2.2. Ocean color dataset

Daily remote sensing reflectance data from two sensors, the Sea-viewing Wide Field-of-view Sensor (SeaWiFS) and MODIS/Aqua, were obtained from the NASA Goddard Space Flight Center (http://oceancolor.gsfc.nasa.gov/). Remote sensing reflectance (*Rrs*) at wavelengths of 412, 443, 490, and 555 nm [Rrs(412), Rrs(443), Rrs(490), Rrs(555)] from SeaWiFS and at 412, 443, 488, and 547 nm [Rrs(412), Rrs(443), Rrs(488), Rrs(547)] from MODIS were analyzed. Several different datasets with various reprocessing versions and levels were used (Table 2.1).

We used empirical Yellow Sea Large Marine Ecosystem Ocean Color Work Group (hereafter YOC) Chl-*a* algorithms for the study area from the SeaWiFS Reprocessing 5.1 (R2005.1) dataset developed by Siswanto et al. (2011). A normalized water-leaving radiance value of 555 nm [nLw(555)] was used to switch from the non-turbid standard algorithm to the turbid algorithm (details in the Appendix). Yamaguchi et al. (2013) modified this switch to produce a smooth image with a linear combination of these algorithms for the low value of nLw(555). Because the YOC Chl-*a* algorithm was based

on an older SeaWiFS R2005.1 dataset and a newer SeaWiFS Reprocessing 2010.0 (R2010.0) dataset is available, linear conversions between the datasets were conducted using band ratios [Rrs(412)/Rrs(490) and Rrs(443)/Rrs(555)]. Furthermore, to make the long time series from SeaWiFS (1998–2010) and MODIS (2002–2010) consistent with one another, we conducted linear conversions of MODIS-Aqua Reprocessing 2009.1/2010.0 (R2009.1/R2010.0) band ratios [Rrs(412)/Rrs(488) and Rrs(443)/Rrs(547)] to SeaWiFS band ratios [Rrs(412)/Rrs(490) and Rrs(443)/Rrs(555)] (details in the Appendix).

To make the 4-km resolution SeaWiFS R2010.0 Level 2 GAC datasets compatible with the 1-km MODIS R2009.1/R2010.0 Level 2 LAC datasets, MODIS data were reduced by four times by averaging four neighboring pixels into one and remapping them to the same dimensions as SeaWiFS (386 × 386 pixels for 17° × 17° in YECS). The newly processed MODIS and SeaWiFS daily datasets were then merged to make more consistent and cloud-free long-term 8-day weekly and monthly Chl-*a* datasets. All merged Chl-*a* data were re-binned to 1° × 1° to reduce the influence of meso-scale variability. We used relatively loose criteria to exclude outliers caused by cloud-edge effects (Vantrepotte and Melin 2009). First, we selected the median value in each grid. Second, assuming a lognormal distribution for the 13-year 8-day weekly and monthly Chl-*a* data in all grids, we removed outliers by excluding data points that were greater than three standard deviations from the mean. These processes enabled 144 ocean grid points to each have data for a 612 8-day weekly time series (14 8-day weeks for 1997 and 598 8-day weeks for 1998–2010). All data processing was conducted using NASA SeaDAS software (version 6.2) and Windows Image Manager (WIM) software (http://www.wimsoft.com/).

2.2.3. Gaussian fitting for phytoplankton blooms

The middle area of the temperate YECS is characterized by a typical spring bloom and a modest fall bloom (Furuya et al., 2003), while the coastal area of the YECS is characterized by a long-duration bloom from spring to autumn (Yamaguchi et al. 2013), and the subtropical area of the Kuroshio is characterized by winter phytoplankton increases (Ueyama and Monger 2005). A flexible curve-fitting procedure was used to model these blooms. First, a modified Gaussian function, which has been widely used to model time series of satellite-derived Chl-*a* (Yamada and Ishizaka 2006; Platt et al., 2007), was selected for the period from winter to summer, when polyp strobilation and larval growth are expected.

Second, the Chl-*a* time series for winter, spring, and summer blooms were selected for fitting. We did not take into account the possible fall bloom because it was not relevant to the analysis of young jellyfish. The Chl-*a* time series was adjusted for each grid so that the largest seasonal blooms would be at the center of each respective time series. Thus, the periods from August 29 to August 28 of the following year, January 1 to July 30, and January 1 to December 31 were used to detect winter, spring, and summer blooms, respectively.

Third, the 8-day weekly time series for Chl-*a*, *CHL(t)*, over one year or half a year were fitted to a modified Gaussian function as follows:

$$CHL(t) = B_s \cdot t + B_i + a \cdot \exp\left\{-\left[\frac{(t - t_p)^2}{2\sigma^2}\right]\right\},$$

where B_s and B_i are the baseline slope and intercept, respectively. $B_s \cdot t + B_i$ and $B_s \cdot t_p + B_i + a$ are baseline and peak Chl-*a*, and t_p, $t_p - 2\sigma$, and $t_p + 2\sigma$ are the times of peak, start, and end of phytoplankton bloom, respectively. The tilted baseline for phytoplankton blooms was used because Chl-*a* before and after the bloom during the analysis periods were significantly different in most of the grids (W-R test: h = 1, p < 0.1, at a 90% confidence level, data not shown). Non-bloom Chl-*a* was defined as the average Chl-*a* of before and after the bloom during the analysis period.

Fourth, for each year in each grid, three types of bloom time series were fitted to the modified Gaussian function described above using the nonlinear least-squares method. If the number of valid values of the time series was less than half of the number for the whole period (<12 8-day weeks for the time series of January 1 to July 30, <22 8-day weeks for the time series of August 29 to August 28 of the following year, and January 1 to December 31), this time-series was removed from the fitting. The quality of the three types of time-series fittings in each grid was assessed using determination coefficients, and the best bloom type was chosen. In some grids, the fitted curve with one negative peak with highest determination coefficient was found. This region was defined as phytoplankton decline region. We were unable to analyze data for a few years in some areas with low determination coefficients ($R^2 < 0.5$).

Fifth, the average timings of phytoplankton blooms for climatological time series from 1998 to 2010 were also fitted the same way, except for the time series of August 29 to August 28 of the following year and January 1 to December 31. For the fitting, B_s was set as 0 (non-tilted baseline) because the difference of Chl-*a* between before

and after the bloom during analysis periods was not significant (W-R test: h = 0, $p > 0.1$, at a 90% confidence level, data not shown).

2.2.4. Statistical analysis

One-sided Wilcoxon rank-sum (W-R) tests (Michael and Proschan 2010) were used to compare SST in JY and NJY, and two-sided W-R tests were used to compare SST in JY and PJY. Linear regression analysis with year was used to obtain long-term trends in monthly SST, non-bloom Chl-*a*, and peak Chl-*a*.

We first identified geographical regions based on Chl-*a* peaks from the Gaussian fitting. Then, to further discriminate spring and summer bloom regions with the geographical and climatological differences in temporal patterns of Chl-*a*, we conducted K-means clustering analysis based on parameters of the phytoplankton bloom (start time, end time, peak time, baseline Chl-*a*, and peak Chl-*a*) (Henson and Thomas 2007; Kim et al., 2009b). This analysis was performed on composites of the 13-year climatological 8-day weekly Chl-*a* time series on the basis of silhouette values (Kaufman and Rousseeuw 1990). These values indicated that the optimum number of clusters for further separation was seven. All statistical analyses and model fitting were performed in MATLAB2012 (www.mathworks.com)

2.3. Results

2.3.1. SST seasonality during 1998–2010

Coastal and middle areas between China and Korea were characterized by large seasonal variations in SST, likely because these areas are shallow and subjected to large quantities of river runoff. The waters of the southeast YECS were characterized by

relatively small seasonal variations in SST, dominated by the warm Kuroshio Current. In winter, the 15°C water was distributed from the Taiwan Strait northeastward along the Zhejiang-Fujian coast (Fig. 2.2a), displaying a distribution pattern similar to that of the tongue-shaped front off the CJE. The 15°C water was found in the center of the YECS, from the northern coast of the CJE to offshore in spring (Fig. 2.2b). SST was quite uniform in the YECS in summer, and higher than 15°C throughout the study region (Fig. 2.2c). In fall, 15°C water was observed from east of the Shangdong Peninsula to south of Korea (Fig. 2.2d).

2.3.2. Interannual variability in SST

We selected seven areas to represent the whole YECS, according to geographic characteristics, not including the Kuroshio and offshore waters where SST was always near or above 15ºC. These areas were distributed from the Chinese and Korean coasts to the middle of the YECS and included the BS, the middle of the northern Yellow Sea (MNYS), the Chinese coast of the southern Yellow Sea (CSYS), the coast of the Shangdong Peninsula (CSDP), the middle of the southern Yellow Sea (MSYS), the Korean coast of the southern Yellow Sea (KSYS), and the CJE (Fig. 2.1).

Interannual variability in SST for all areas in the YECS was approximately 0–5°C during spring to summer, and smaller than the seasonal variability (Fig. 2.3). SST decreased significantly ($r < –0.5$, $p < 0.05$) in April, May, and June in the MSYS from 1998 to 2010 (Fig. 2.3e). A significant decrease ($r < –0.5$, $p < 0.05$) was also observed in March, May, and June in the CSDP (Fig. 2.3d); however the decrease was only significant in March, May, and June in the CSYS, MNYS, and BS, respectively (Fig. 2.3a-c).

The SST was much lower in NJY than in PJY and JY from spring to early summer, with differences of approximately 0–5°C (Fig. 2.4). However, the differences in SST in JY and PJY were not significant (W-R test: h = 0, p > 0.1, at a 90% confidence level) in most of the YECS. The range of the differences was approximately 0–1.5°C from spring to early summer. Longer time series (1985–2007, data not shown) with additional SST datasets from AVHRR showed significant increase ($r > 0.5$, $p < 0.05$, 1.50ºC) during the 23 years in the majority of the YECS (MSYS, CSYS, CJE, MNYS and BS) throughout spring and early summer. The low SST in NJY caused the significant decrease from 1998 to 2010 in the YECS. The long-term results indicate that the SST increased significantly with a maximum in PJY and JY during spring and early summer in recent decades.

The spatial distribution of the SST difference between JY and NJY also indicates that SST in NJY was lower than in JY in large areas of YECS from April to June (Fig. 2.5). In March, SST in NJY was only slightly lower (0–1.5°C) than in JY, and the difference was not statistically significant at a 90% confidence level (h = 0, $p > 0.1$) throughout the YECS, except in two grids (Fig. 2.5a). In April, SST in NJY was significantly lower (2–5°C) than in JY (W-R test: h = 1, $p < 0.1$) in CJE and its adjacent waters (Fig. 2.5b). In May, SST in NJY was significantly lower (1.5–2°C) than in JY in a large area of the YECS, including the CSYS, MSYS, and Huanghe River estuary of the BS (Fig. 2.5c). In June, SST in NJY was significantly lower (2–3°C) than in JY (h = 1, $p < 0.1$) in most parts of the BS, CSYS, MSYS, and KSYS (Fig. 2.5d).

2.3.3. Phytoplankton bloom climatology

Based on the seasonal peaks in Chl-*a*, we identified three (winter, spring, and summer) major bloom regions and one summer decline region in the YECS (Fig. 2.6a). The winter bloom region was distributed in the southeast subtropical region with low seasonality, influenced by the Kuroshio. The spring bloom region covered most of the YECS, specifically in the middle regions deeper than 50 m. The summer bloom region mainly occupied the coastal area of the YECS, with the boundary corresponding well with the 50-m isobath, extending from the coast of Fujian Province to most of the BS and the Korean coast. The summer decline region was confined to the coast of Shangdong Peninsula.

In the winter bloom region, seasonal and interannual variability of Chl-*a* was small (Fig. 2.7a), with the lowest baseline (< 0.1 mg m^{-3}) and peak (< 0.25 mg m^{-3}). In the spring bloom region, seasonality was larger, with the tilted baseline and peak of 0.5–0.7 and 1.2 mg m^{-3}, respectively (Fig. 2.7b). Chl-*a* in coastal regions of the YECS exhibited a distinct seasonal cycle, with a peak in midsummer. The baseline and peak in coastal regions were highest, with values of 1.8 and 3.1 mg m^{-3}, respectively (Fig. 2.7c). The interannual variability of Chl-*a* in the summer bloom region, represented by standard deviations (0.23–0.73 mg m^{-3}), was large around the peak of the bloom. In the summer decline region, the peak was negative with a fitted Gaussian function (Fig. 2.7d).

The start time of the summer bloom was late in the CJE, CSYS, and BS in May or June (Fig. 2.8a). The end time of the winter and spring blooms was from May to June around the Okinawa Islands and March to April in the middle of YECS (Fig. 2.8b). In the coastal regions, the end of the bloom occurred from early September in the CSYS to late November in the CJE, BS, and KSYS. The peak of the phytoplankton bloom

generally occurred in mid-January for most of the southeast, in early or mid-April for the middle of the YECS, and in late July or early August for the coast of the YECS (Fig. 2.8c). In the subtropical Okinawa region, a long and low-intensity winter increase in Chl-*a* was observed (Fig. 2.8d, f). In contrast, bloom duration tended to be shorter in the middle YECS compared with other regions (Figs. 2.7b, 8d). Non-bloom Chl-*a* were extremely low in the Okinawa region and generally high in the middle and coastal regions of the YECS, with a maximum in BS (Fig. 2.8e). High peak (>4 mg m^{-3}) was found in CJE and its adjacent waters, CSYS, KSYS, and in most parts of the BS (Fig. 2.8f).

2.3.4. Interannual variability in the timing of phytoplankton blooms and the Tsst15

We focused on the YECS where SST varied around 15°C and excluded the Kuroshio and offshore waters (Fig. 2.6b). A cluster analysis of the 13-year Chl-*a* time series data revealed seven distinctive regions with significant different seasonal cycles of Chl-*a*; BS, MNYS, CSYS, CSDP, MSYS, KSYS, and CJE. The same abbreviated names were used for each region as the name of the SST study because the areas of investigated SST in Section 3.2 were located near the centers of each region (Fig. 2.1).

A high summer peak with a long bloom period was observed for most of the years in the BS, CSYS, KSYS, and CJE (Fig. 2.9, Table 2.2). A lower Ch-*a* during shorter spring bloom was observed in the majority of the years in MNYS and MSYS. The Chl-*a* peak was negative in midsummer in the CSDP. Significant increases ($r > 0.5$, $p < 0.05$) in both non-bloom and peak Chl-*a* from 1998 to 2010 were observed in most regions of the YECS (Fig. 2.9, Table 2.2). The increases in non-bloom and peak Chl-*a* were 55.0, 35.8, 18.0, 35.7% and 80.0, 60.0, 55.0, 38% in BS, CSYS, MSYS, KSYS,

respectively. Both non-bloom and peak Chl-*a* also increased in the CJE (9.5 and 8–10%, respectively).

The start and end times of the blooms exhibited considerable interannual variability (more than six 8-day weeks) in BS, CSYS, KSYS, and CJE (Fig. 2.9, Table 2.2). The timing of phytoplankton blooms exhibited less interannual variability (within six 8-day weeks) in MNYS and MSYS. In the CSDP, the start and end times of the phytoplankton decline exhibited considerable interannual variability (more than six 8-day weeks). The Tsst15 exhibited similar interannual variability in almost all regions, generally within two 8-day weeks: this was near the start of the bloom in the BS, CSYS, KSYS, and CJE regions, and near the end of the bloom in the MNYS and MSYS regions in most years (Fig. 2.9, Table 2.2). The Tsst15 was also close to the start of the phytoplankton decline in the CSDP in all years (Fig. 2.9d).

2.4. Discussion

In this study, three hypotheses (temperature, eutrophication, and match–mismatch) were examined to explain the jellyfish outbreaks after 2002, and their absence in 2008 and 2010, using satellite SST and Chl-*a*.

2.4.1. Temperature hypothesis

Global warming is considered an important factor affecting increases in jellyfish outbreaks (Purcell et al., 2007; Richardson et al., 2009). Our analysis indicated that SST significantly increased during the 23 years from 1985 to 2007 in spring and early summer. This finding was consistent with previous results, such as those published by Lin et al. (2005), who observed that the regional mean temperature in the Yellow Sea

increased by 1.7ºC from 1976 to 2000. The maximum SST in PJY and JY indicated that the long-term increase in SST generally corresponded to recent increases in jellyfish outbreaks.

Uye (2008) speculated that warmer temperatures may induce higher birth rates of *N. nomurai* medusae by accelerating asexual reproduction, based on the results of laboratory experiments (Kawahara et al. 2006). Our analysis of the SST in YECS based on satellite data also indicated that the high temperature in YECS was favorable for *N. nomurai*. This result supports the temperature hypothesis.

The temperature hypothesis can also explain the lack of *N. nomurai* outbreaks in 2008 and 2010 (NJY), when the SST was as low as in the 1980s. Because *N. nomurai* has a short lifespan (one year), the fluctuation of abundance could be caused by short-term climatic variations, as has been suggested for *Aurelia aurita* and *Cyanea lamarckii* in the North Sea (Lynam et al., 2004; Lynam et al., 2005). The absence of *N. nomurai* outbreaks in 2008 and 2010 may be attributable to unfavorable conditions caused by the low temperatures associated with the climate variation. However, no jellyfish outbreak occurred in PJY, even though the SST was as high as in JY.

It is still not clear how temperature control the outbreak. One possibility is that the match/mismatch of the prey abundance to young jellyfish is controlled by temperature. However, the match/mismatch to phytoplankton bloom was not clearly related to interannual variation of jellyfish outbreaks, if the phytoplankton bloom was an indicator of high zooplankton abundance.

Temperature might directly influenced physiology of ephyrae, further, the survival of ephyrae because ephyrae probably act through its own physiological response to

temperature in certain time, like a response to the temperature-sensitive "timer" (Fuchs et al., 2014). It is possible that high survival of ephyrae was attained in the certain time of warmer years when the temperature reach 15^{o}C earlier. It needs further verification in future to understand whether this hypothesis is true or not.

2.4.2. Eutrophication hypothesis

Our results revealed that both the non-bloom and peak Chl-*a* increased significantly from 1998 to 2010, with a great increase observed in coastal regions (Fig. 2.9, Table 2.2). This indicates that eutrophication was more severe in recent years (JY and NJY), as the nutrient loading continued from land (Zhou et al. 2008; Gao and Zhang 2010). The high food availability resulting from more eutrophic conditions in coastal regions of the YECS, especially in the CSYS, KSYS, and BS, may favor polyp strobilation and survival of ephyra in JY. Conversely, less eutrophic conditions limit polyp strobilation, likely resulting in lower survival of ephyra and thus less recruitment of *N. nomurai* medusae in PJY. The mechanism of less eutrophic condition was still not clear; probably this condition makes less contribution to flagellate bloom, which favored fish other than jellyfish. The low eutrophication level was probably related with increased light penetration, which may alter the feeding environment to benefit visually feeding fish over the non-visual jellyfish. Whether less eutrophication directly or indirectly influences jellyfish need further investigation.

Our study also indicated that high eutrophic conditions in NJY did not correspond to high jellyfish abundance, indicating that eutrophication was necessary but not sufficient for jellyfish outbreaks. As explained in Section 2.4.1, the low temperature is a

probable cause of unfavorable conditions for *N. nomurai* even in a eutrophic environment.

Kawahara et al. (2006) speculated that the ecosystem changes associated with eutrophication may be responsible for the enhancement of giant jellyfish populations. We found that phytoplankton, which is food for zooplankton, increased significantly from PJY to JY in YECS. This result indicates that the ecosystem is changing in YECS associated with eutrophication (Kawahara et al. 2006; Siswanto et al. 2008). The increase in phytoplankton due to eutrophication in combination with higher temperatures due to climate change probably led to long-term increases in jellyfish outbreaks.

2.4.3. Match–mismatch hypothesis

High temperatures may act directly on polyps to enhance strobilation (Kawahara et al. 2006). Alternatively, several studies suggested an indirect influence of temperature through alteration of the timing of phytoplankton blooms to synchronize with the period of rapid ephyral growth (Platt et al., 2003). We found that the ephyral stage, as indicated by the Tsst 15, was always near the start of the bloom in coastal areas, while it was always near the end of bloom in middle areas. Furthermore, variability in the start and end times of phytoplankton blooms did not correspond to timings of the ephyral stage in warmer JY and colder NJY in each region. In particular, the delay in the Tsst15 did not result in a mismatch with phytoplankton blooms in NJY. A change in the physiology of jellyfish larvae due to low SST was more likely to have resulted in low survival of ephyra in NJY (Kawahara et al., 2006; Purcell et al., 2009).

Our analyses also indicated that the timing of phytoplankton seasonal blooms differed greatly between coastal and middle areas (Fig. 2.9). If the timing of phytoplankton blooms corresponds to jellyfish prey abundance, matches and mismatches between the timings of phytoplankton blooms and the Tsst15 were observed in all years in the coastal (BS, CSYS, KSYS, and CJE) and middle (MNYS and MSYS) areas of the YECS, respectively (Fig. 2.9). The difference indicates that survival of ephyra may differ between middle and coastal regions, although no information is available at present.

The main prey of *N. nomurai* medusae are small copepods and gastropod larvae (size <1 mm) that may directly feed on phytoplankton (Uye 2008). According to Lee et al. (2008), the ephyrae of *N. nomurai* could feed on prey similar to that of large adult medusae. Thus, the timing of phytoplankton blooms may affect survival of ephyra through a complex bottom-up process (Gremillet et al. 2008). In general, a time lag occurs between phytoplankton blooms and increases in zooplankton abundance (Kiorboe and Nielsen 1994; Zervoudaki et al. 2009).

Kang et al. (2012) suggested that copepod abundance increases from spring until the seasonal peak in summer along the Korean western coast, increases from February with the seasonal peak in April, and then decreases until August in the north East China Sea near the Tsushima Strait. If we assume that the results of Kang et al. (2012) in the Korean coast and in the northern East China Sea are applicable to the YECS coastal and middle regions, the Tsst15 (ephyral stage) corresponded to the copepod abundance peak in coastal regions and the minimum in the middle regions. This is consistent with our results for phytoplankton blooms: match and mismatch in coastal and middle regions,

respectively. However, Kang et al. (2012) only investigated average bimonthly zooplankton data from February to December in Korean waters. Temporal and spatial data limitations obviously restrict interpretation of the match–mismatch between zooplankton abundance and the jellyfish ephyral stage. More *in situ* data are required to validate the details of the match–mismatch of *N. nomurai* to prey abundance.

2.5. Conclusions

Using 13 years of satellite (AVHRR, SeaWiFS, MODIS-Aqua) SST and Chl-*a* data, we characterized long-term environmental variables related to interannual variability of *N. nomurai* outbreak in the YECS for the first time. Three hypotheses (temperature, eutrophication, and match–mismatch) were examined to explain the variability in jellyfish outbreaks in the YECS. Our results indicated that the long-term increases in *N. nomurai* outbreaks and the recent absence may be driven by anthropogenic factors and climate change (Fig. 2.10).

Increased eutrophic conditions and the warming of seawater in late spring and early summer were favorable to, and a necessary condition for, the long-term increase in *N. nomurai* outbreaks in JY. However, significantly lower SST in NJY compared with JY indicates that SST was an important factor lowering the proliferation of *N. nomurai* in NJY through effects on survival of ephyra. Timing of phytoplankton blooms varied interannually and spatially, and their match and mismatch to the timing of SST reaching 15°C was not corresponded to the long-term increases in *N. nomurai* outbreaks and the recent absence. Instead, survival of ephyra may differ in middle and coastal areas. Once ephyra establishes its population with high survival rates, the fast growth from ephyra to

young medusae under favorable conditions (temperature, food) probably could lead to a later jellyfish outbreak.

Table 2.1 Satellite data used in this study

Satellite data sets	Sensor	Wavelength(nm)	Product	Resolution	Version	Year
SST	AVHRR	-	-	4 km	5.0	1998-2002
	MODIS	-	Level 3	4 km	-	2003-2012
Remote Sensing Reflectance (Rrs)	SeaWiFS	412, 443, 490, 555	GAC Level 2	4 km	R2005.1	1998-2007
	SeaWiFS	412, 443, 490, 555	GAC Level 2	4 km	R2010.0	1998-2010
	SeaWiFS	412, 443, 490, 555	MLAC Level 2	1 km	R2010.0	2002-2004
	MODIS	412, 443, 488, 547	LAC Level 2	1 km	R2009.1	2002-2008
	MODIS	412, 443, 488, 547	LAC Level 2	1 km	R2010.0	2009-2012

Table 2.2 Interannual variability of non-bloom Chl-*a*, peak Chl-*a*, timings of phytoplankton blooms and Tsst15

Locations	Chl-*a* pattern	Start time	End time	Non-bloom Chl-*a* (mg m^{-3})	Peak Chl-*a* (mg m^{-3})	13 years increasing trend in non-bloom Chl-*a*	13 years increasing trend in peak Chl-*a*	Tsst15
BS	Summer bloom	Early Mar. to early Jun.	Early Oct. to middle Nov.	1.9~3.1	2.5~4.5	55% ($r = 0.884$, $p < 0.05$), with 19% from PJY to JY	80% ($r = 0.882$, $p < 0.05$), with 31% from PJY to JY	Middle to late May, just after start time
MNYS	Spring bloom	Early Jan. to middle Feb.	Early May to late Jun.	1.0~1.7	1.8~3.3	-	-	Late May to early Jun., just before or after end time
CSYS	Summer bloom	from middle May to middle Jul. except 2009	Middle Aug. to late Oct.	1.4~2.1	2.0~3.2	35.8% ($r = 0.831$, $p < 0.05$), with 14% from PJY to JY	60% ($r = 0.55$, $p < 0.05$), with 18% from PJY to JY	Early May to middle May, just before start time except 2009
MSYS	Spring Bloom	Middle Feb. to early Apr.	Early May to late May	0.8~1.1	1.5~2.3	18% ($r = 0.61$, $p < 0.05$), with 4% from PJY to JY	55% ($r = 0.66$, $p < 0.05$), with 8.2% from PJY to JY	Late May to early Jun., just before or after the end time
KSYS	Summer bloom	Early May to late Aug.	Late Sep. to early Dec.	1.5~2.2	2.5~8.6	35.7% ($r = 0.85$, $p < 0.05$), with 14.5% from PJY to JY	38% ($r = 0.75$, $p < 0.05$), with 26% from PJY to JY	Late May to early Jun., just before or after the start time
CJE	Summer bloom	Middle Feb. to early Jun.	Middle Aug. to late Dec.	0.7~1.5	2.0~3.8	9.5% without significant trend, with 5% from PJY to JY	8-10% without significant trend, with 5% from PJY to JY	Middle to late Apr., just after start time except 1998-1999

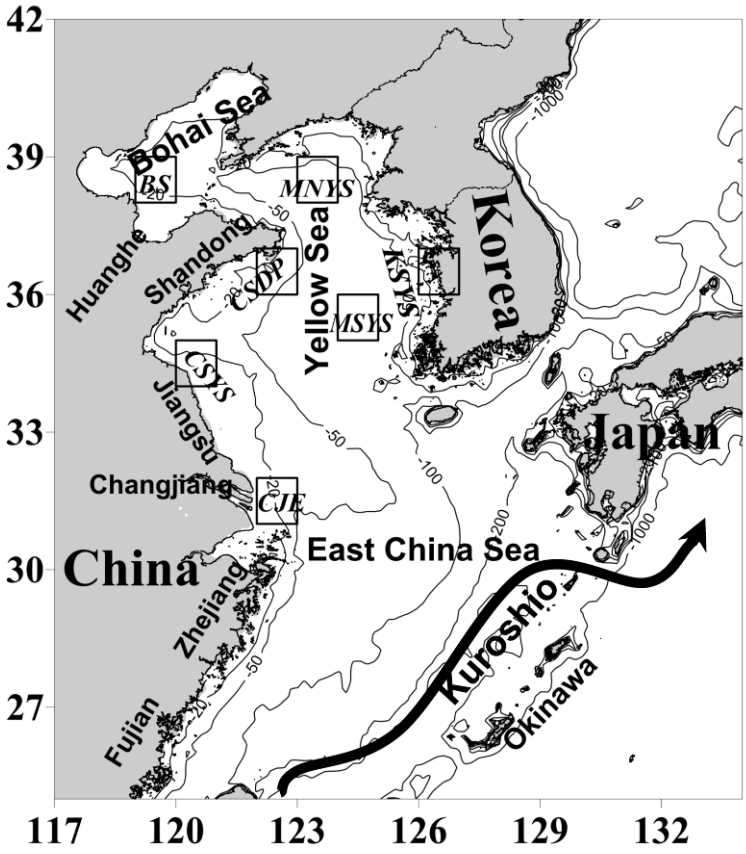

Fig. 2.1 Bathymetry of the Bohai Sea, Yellow Sea, and East China Sea. Seven 1 × 1° boxes represent areas for SST investigation: the Bohai Sea (BS), the middle of the northern Yellow Sea (MNYS), the Chinese coast of the southern Yellow Sea (CSYS), the coast of the Shangdong Peninsula (CSDP), the middle of the southern Yellow Sea (MSYS), the Korean coast of the southern Yellow Sea (KSYS), and the Changjiang River estuary (CJE).

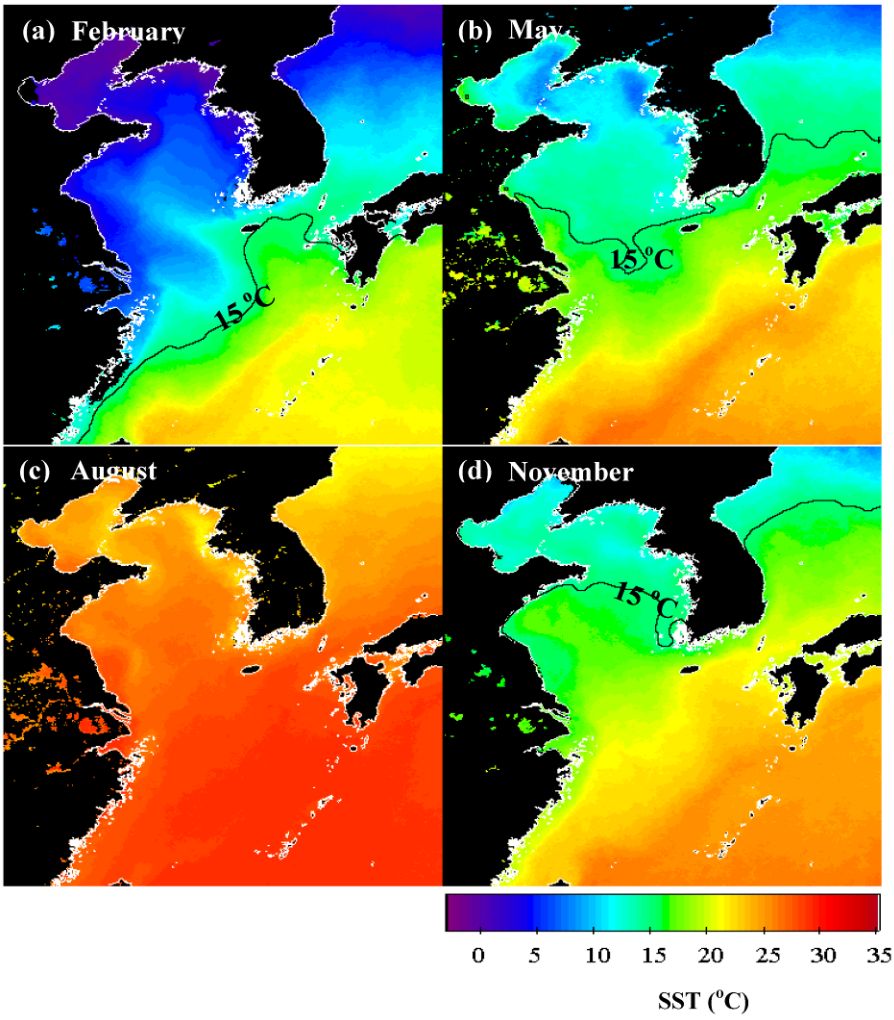

Fig. 2.2 Thirteen-year climatology SST data. (**a)** February, (**b)** May, (**c)** August, and (**d)** November represent winter, spring, summer, and autumn, respectively. Lines indicate the isotherm of 15°C SST.

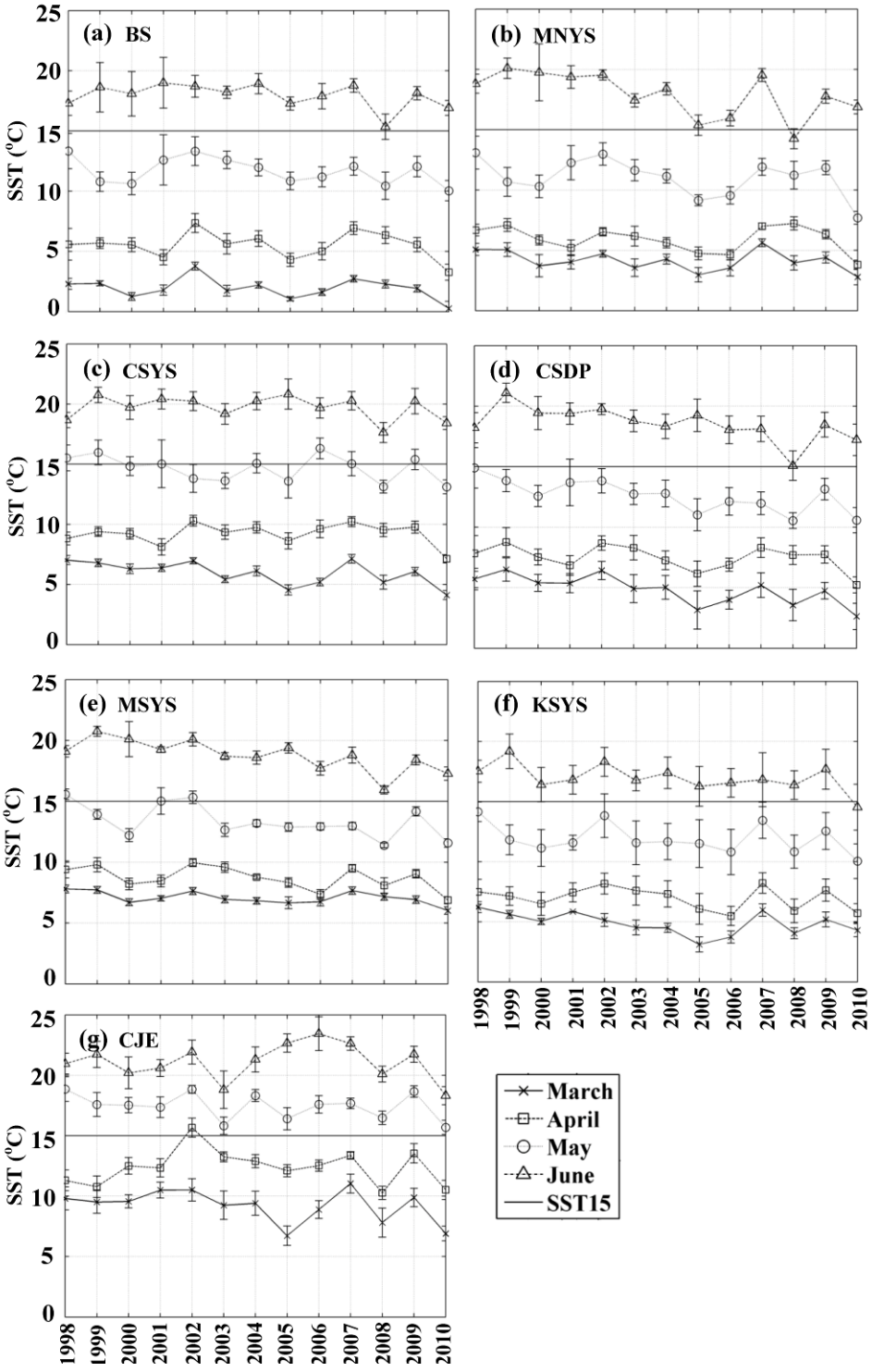

Fig. 2.3 Interannual variability in monthly SST during spring to summer (March to June) in **(a)** BS, **(b)** MNYS, **(c)** CSYS, **(d)** CSDP, **(e)** MSYS, **(f)** KSYS, and **(g)** CJE. Error bars indicate standard deviations in each box. Black lines indicate the isotherm of 15°C SST. The seven areas are marked in Fig. 1.

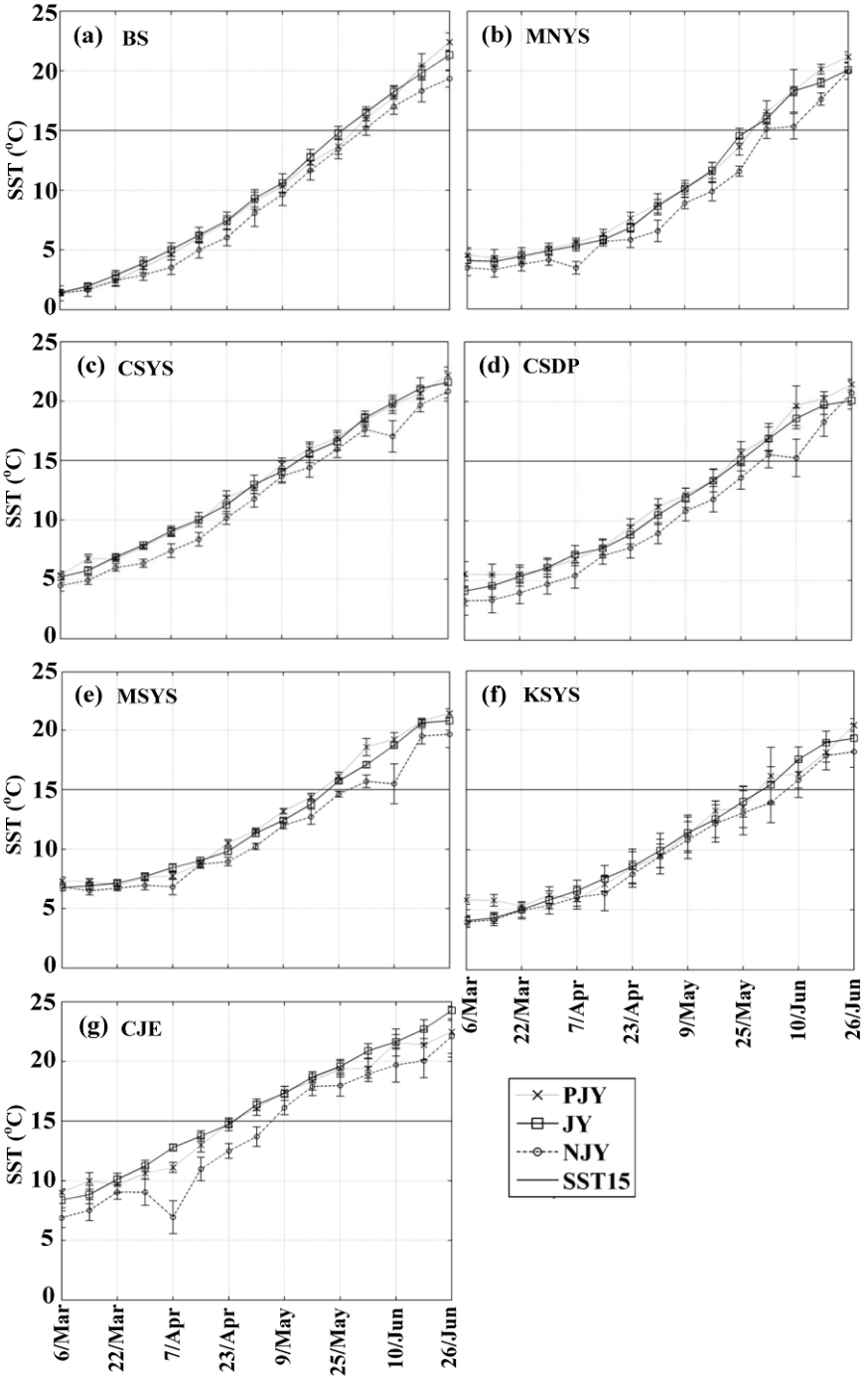

Fig. 2.4 8-day weekly SST time series in PJY, JY, and NJY during spring to summer (March to June) in **(a)** BS, **(b)** MNYS, **(c)** CSYS, **(d)** CSDP, **(e)** MSYS, **(f)** KSYS, and **(g)** CJE. Error bars indicate standard deviations in each box. Black lines indicate the isotherm of 15°C SST. The seven areas are marked in Fig. 1. The corresponding date in ordinary years of the Julian day calendar is shown in the abscissa.

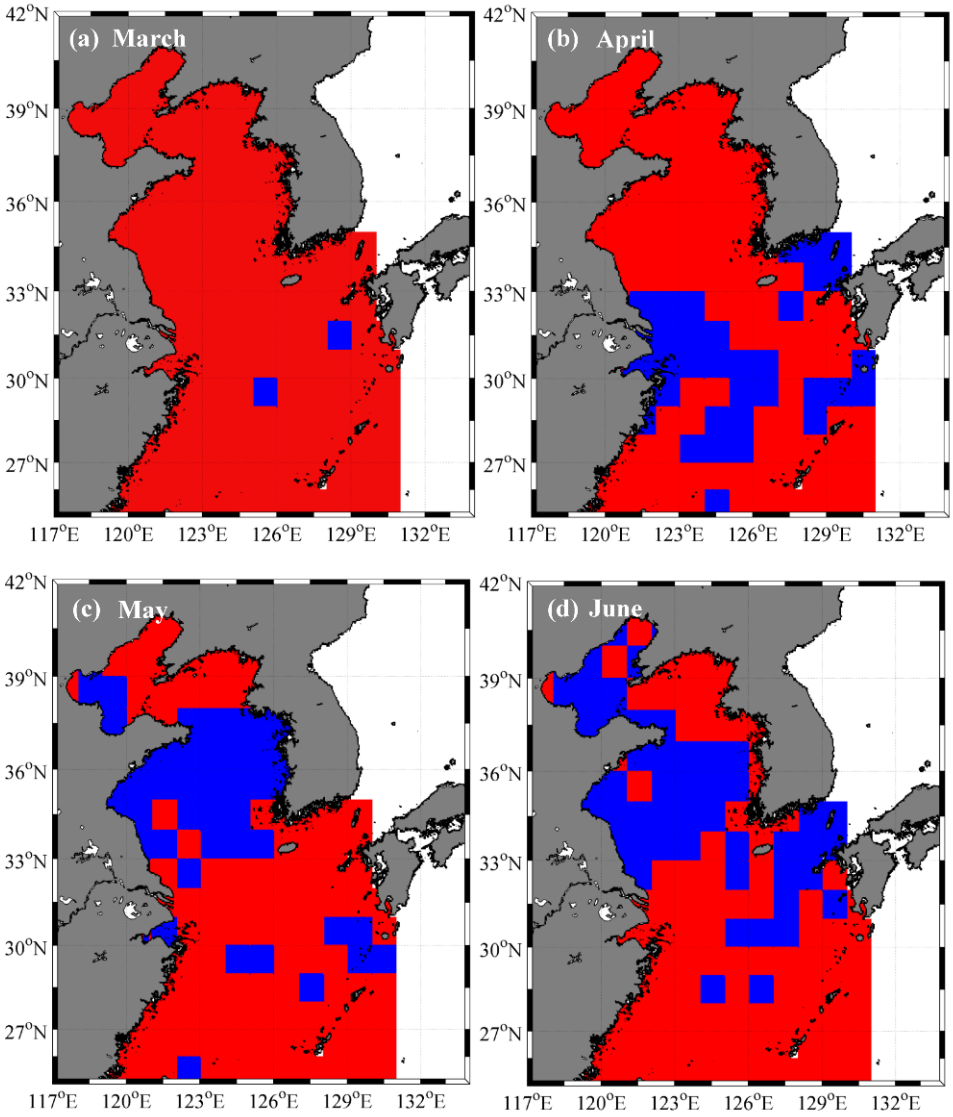

Fig. 2.5 Spatial distribution of differences between SST in NJY and JY during **(a)** March, **(b)** April, **(c)** May, and **(d)** June. Blue and red colors indicate whether SST in NJY was significantly lower (h = 1, $p < 0.1$) or not (h = 0, $p > 0.1$), respectively, from values in JY.

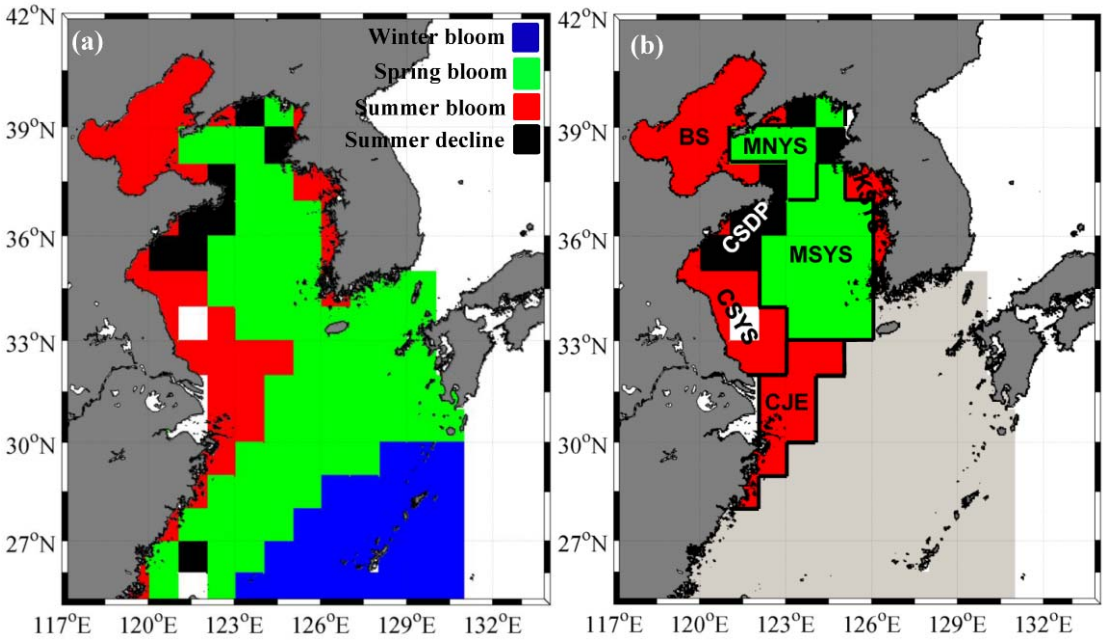

Fig. 2.6 (**a)** Spatial distribution of the temporal pattern of Chl-*a*. Blue, green, red, and black represent the winter bloom, spring bloom, summer bloom, and summer decline regions, respectively. The white grids with few valid satellite data were omitted from further study. (**b)** Detailed separation by K-means clustering of spring bloom and summer bloom regions based on geographical and climatological differences in temporal patterns of Chl-*a*. The spring bloom region was separated into the MNYS and MSYS regions, and the summer bloom region was separated into the BS, CSYS, KSYS, and CJE regions. The light-gray region was omitted from further study because of high SST (always near or above 15ºC)

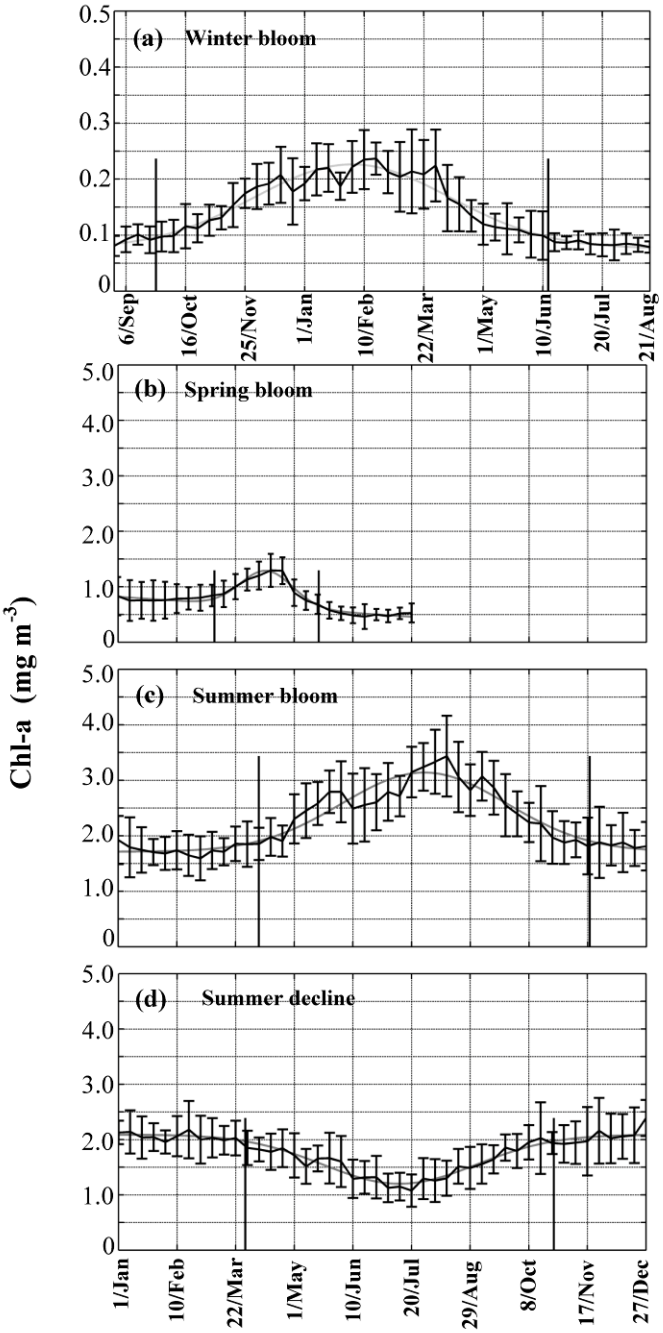

Fig. 2.7 The 13-year mean Chl-*a* seasonality in regions of the (**a)** winter, (**b)** spring, and (**c)** summer blooms, and **(d)** the summer decline from 1998 to 2010, with means ± standard deviations of the peak, bloom timing, bloom duration, and baseline. Black vertical lines indicate start and end times of the bloom, and thick gray lines indicate the fitted curve. The corresponding date in ordinary years of the Julian day calendar is shown in the abscissa.

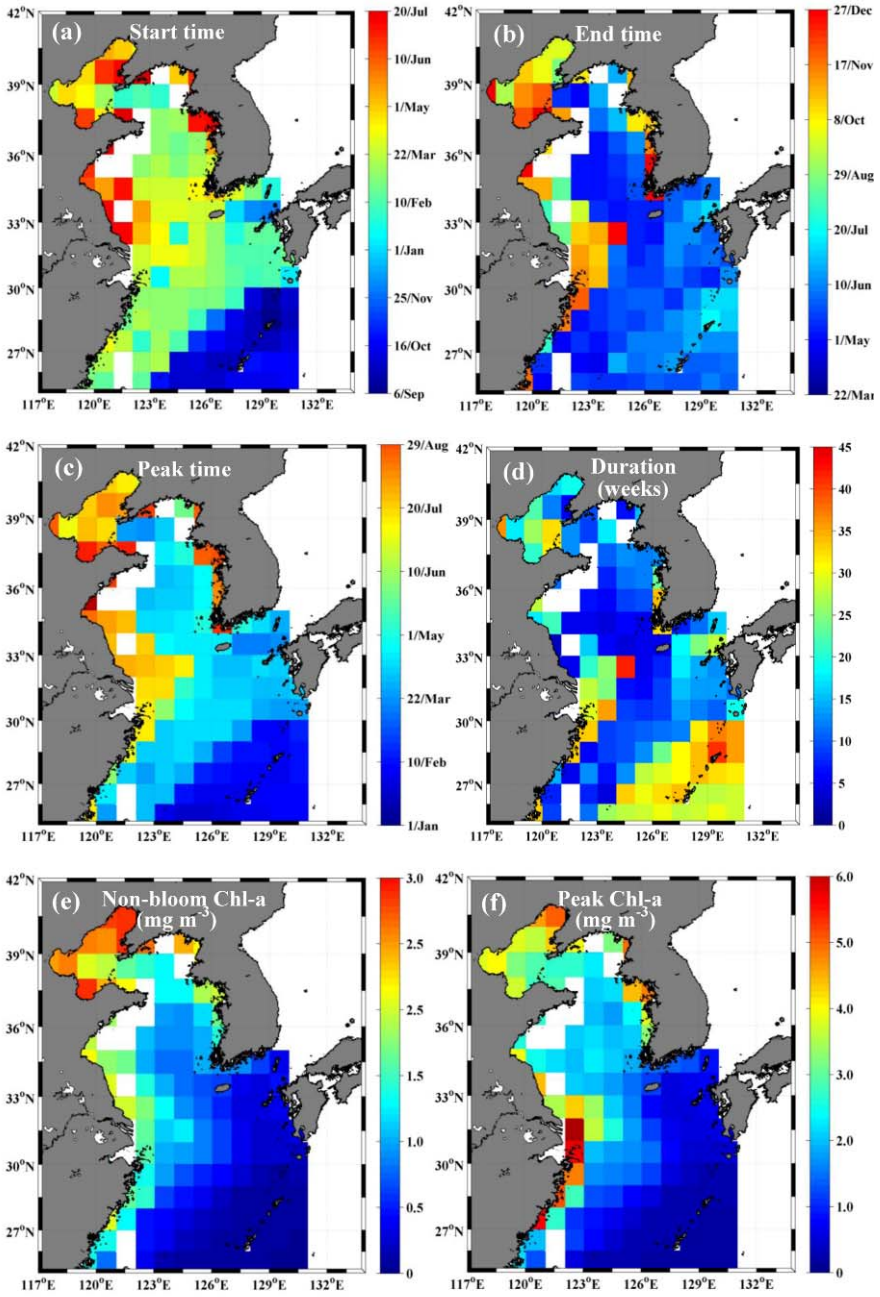

Fig. 2.8 (**a)** Start time, (**b)** end time, (**c)** peak time, (**d)** duration, (**e)** average Chl-*a* during the non-bloom period (non-bloom Chl-*a*), and **(f)** peak Chl-*a* from 13-year mean Chl-*a* data. Summer decline regions in CSDP are excluded (white).

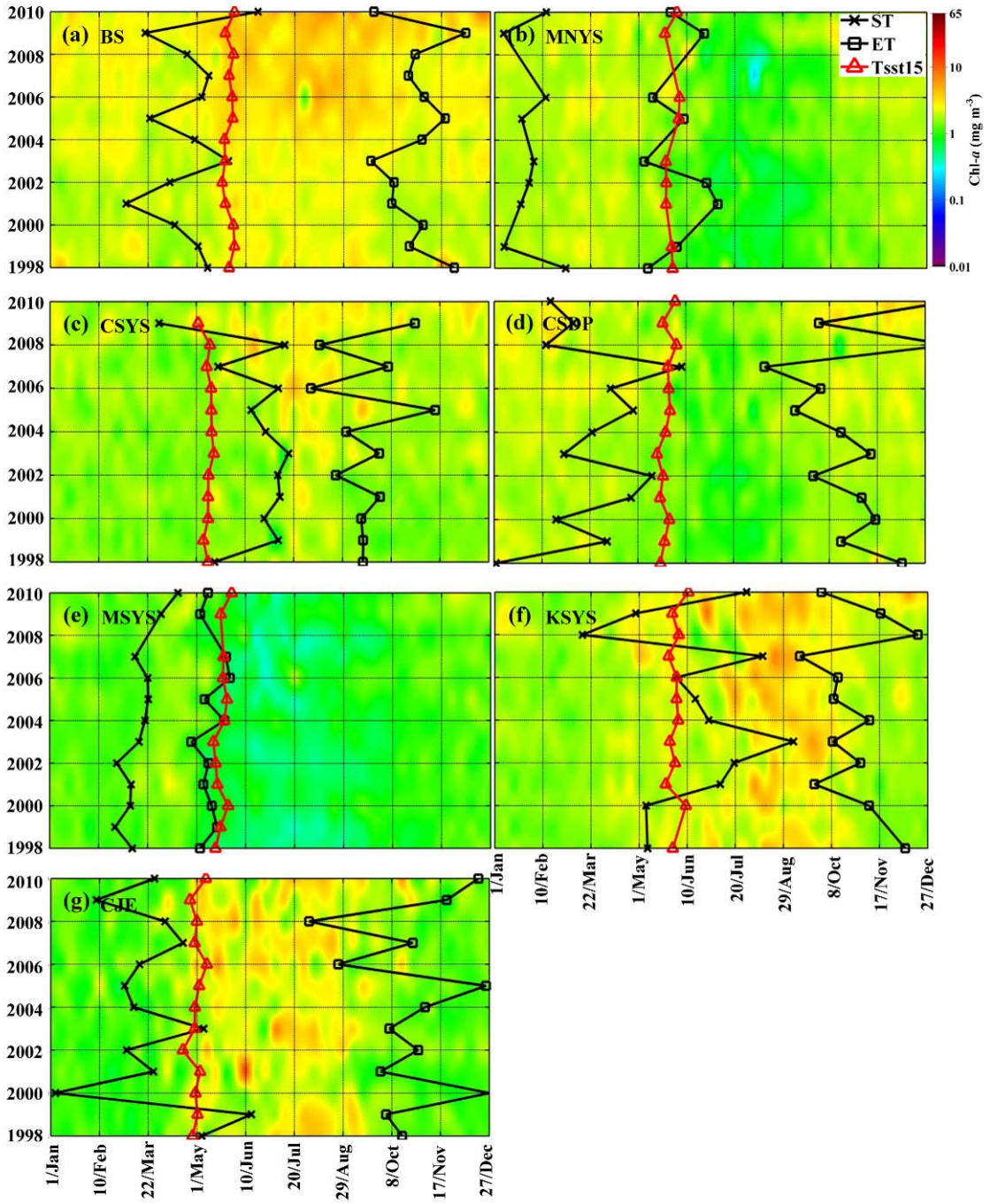

Fig. 2.9 Interannual variability in phytoplankton blooms and the Tsst15 in **(a)** BS, **(b)** MNYS, **(c)** CSYS, **(d)** CSDP, **(e)** MSYS, **(f)** KSYS, and **(g)** CJE. Black crosses and squares indicate the start time (ST) and end time (ET), respectively, and red triangles indicate the Tsst15. The corresponding date in ordinary years of the Julian day calendar is shown in the abscissa.

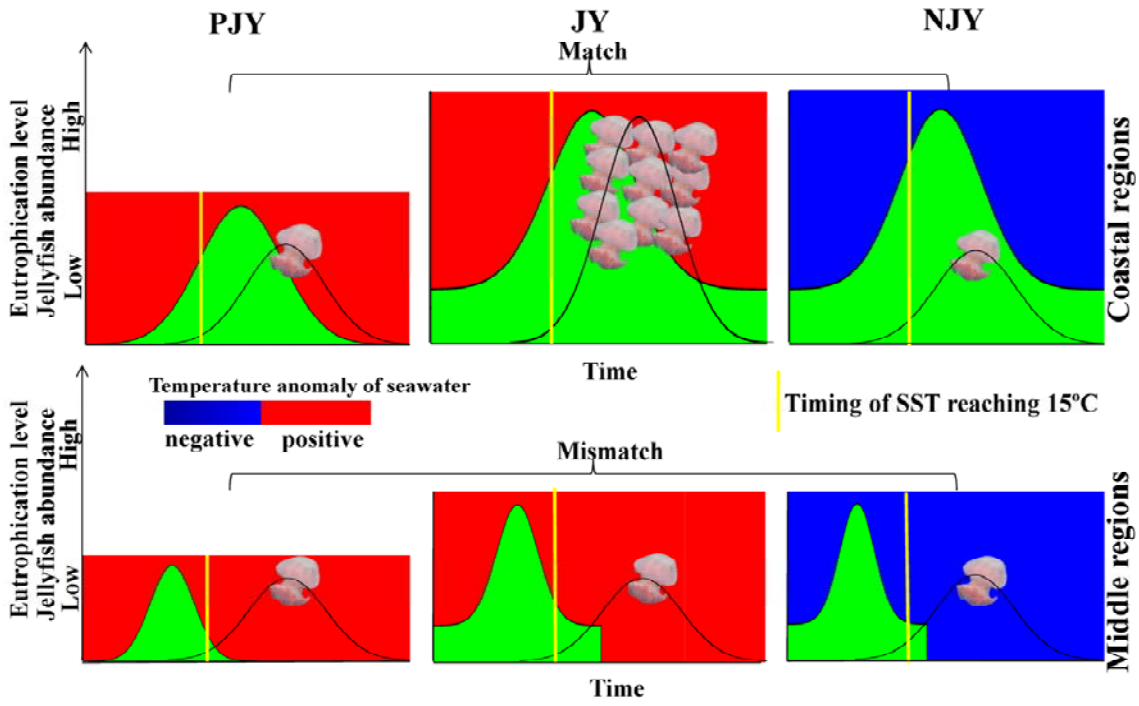

Fig. 2.10 Conceptual diagram of the temporal relationship between jellyfish outbreaks and environmental variables. In periods when jellyfish and phytoplankton biomass overlap or when eutrophication occurs, the larvae will have adequate food and therefore enhanced survival probability. In years when the water temperature is warmer/colder, the jellyfish larvae will have high/low survival rates, leading to a later presence/absence of jellyfish outbreaks. Green indicates phytoplankton biomass; black curved lines indicate jellyfish abundance in PJY, JY, and NJY; red indicates that SST was temporally higher in PJY and JY than in NJY; and blue indicates that SST was lower. Yellow lines indicate the Tsst15.

Chapter 3: Transport of the giant jellyfish *Nemopilema nomurai* from its potential source in the Yellow Sea and East China Sea revealed by field observation, satellite data, and particle-tracking experiments

3.1. Introduction

With its high abundance, the giant jellyfish *Nemopilema nomurai* has in recent decades been a serious problem for the marine ecosystem and for the dependent economies of countries of northeast Asia, especially Japan, China, and Korea (Kawahara et al., 2006; Uye, 2008; Dong et al., 2010; Zhang et al., 2012). Extensive and consecutive outbreaks have occurred in the Yellow Sea (YS), East China Sea (ECS), and the Sea of Japan each year since 2002, except for 2008, 2010, and 2011 (Kawahara et al., 2013; Xu et al., 2013). The origins and causes of these giant jellyfish outbreaks, as well as their distribution, are of great concern to the scientific community. It has been suggested that eutrophication and climate change as well as overfishing and habitat modification (Purcell et al., 2007; Purcell, 2012; Uye, 2008, 2011) are probable causes of outbreaks, and these suggestions have been supported by laboratory experiments (Kawahara et al., 2006, 2013) and a recent satellite study (Xu et al., 2013). Coastal areas of the YS and ECS, with suitable substrate resulting from the development of aquaculture (Dong et al., 2010), eutrophic waters due to increased nutrients (Uye, 2008; Xu et al., 2013), and opportunities for ecological niches because of overfishing (Uye, 2008), have been hypothesized to be sources in many studies (Kawahara et al., 2006; Uye, 2008; Yoon et al., 2008), even though polyps have not been found in nature. The reported appearance of young medusae in the Tsushima Strait and Jeju area in June (Kawahara et al., 2006; Yoon et al., 2008), the capture of relatively large adults (diameter >30 cm) in the Sea of Japan in August, and the fact that ephyrae have not

been discovered in these areas suggest the advection of young medusae from the coasts of the YS and ECS by circulation. Indeed, *N. nomurai*, with its weak swimming and migrating behavior, can be a good indicator of water mass movement because its temporal and spatial distributions generally depend on its interactions with horizontal circulations (Honda et al., 2009).

Freshwater runoff, especially from the Changjiang River, and oceanic currents such as the Kuroshio and Taiwan warm currents (KWC and TWC, respectively) induce major circulation patterns in the YS and ECS (Zhang et al., 2007; Siswanto et al., 2008; Yuan et al., 2008; Kim et al., 2009). Seasonal currents and local currents are also characteristics of YS and ECS circulation. The Yellow Sea Warm Current (YSWC), which is the main component of YS circulation in winter, transports warm and high-salinity water from the southeast to the middle of the YS along the trough (Moon et al., 2009). This northward current is balanced by southward-flowing coastal currents along the coasts of China and Korea, including the Yellow Sea Coastal Current (YSCC) and the Korea Coastal Current (Yuan et al., 2008; Moon et al., 2009). The YSCC was traditionally thought to flow southward throughout the entire year (Wang et al., 2013); however, recent numerical and field studies suggest that the YSCC flows northward along the Jiangsu coast during summer (Liu et al., 2009; Qiao et al., 2011). Changjiang Diluted Water (CDW), which is characterized by southward flow along the Zhejiang and Fujian coasts of China in winter and eastward and northeastward flow toward Jeju Island in summer, plays a critical role in sustaining YS and ECS continental-shelf fisheries resource (Gong et al., 2011). A circulation pattern, characterized by southward flow of the YSCC in early spring and the spreading of CDW in early summer, was adopted by Yoon et al. (2008) to explain the advection and distribution of young

jellyfish. They surmised that ephyrae are transported southward from the YS coast to the area near the mouth of the Changjiang in early spring and then in May drift with the spreading CDW, which is driven by southerly winds.

This horizontal movement of jellyfish was also supported by Kawahara et al. (2006), who further estimated that liberation of ephyrae (the initial free-swimming larval stage of a jellyfish asexually produced from the benthic stage, polyp) may take place in spring and early summer when water temperature in the coastal areas of the YS and ECS increases from 10°C to 20°C based on the size and growth rate of jellyfish caught near Gunsan, Korea, and in the Tsushima Strait in June and July, respectively. A temperature of 15°C is critical for allowing released ephyrae to grow and for producing the highest cumulative strobilation rate for *N. nomurai* (Kawahara et al., 2013). The timing of the 15°C temperature and thermal elevation from below 15°C to higher temperatures has generally occurred in about May and early June in coastal areas of the YS and ECS (Xu et al., 2013). A recent survey confirmed a possible source of the jellyfish in coastal areas near Jiangsu by the presence of ephyrae off of Jiangsu in late May 2011 (Toyokawa et al., 2012). These previous studies indicate that circulation and hydrological processes play important roles in the spread and distribution of ephyrae or young medusae (the free-swimming stage after ephyrae) in the YS and ECS when the strobilation temperature is attained in spring and early summer. However, it remains unclear how the ephyrae and young medusae interact with the water mass and circulation from the source and how these influence the subsequent path and distribution of young medusae in the offshore areas of the YS and ECS.

The main objectives of this study were to investigate the transport of ephyrae and young medusae and its relationship with seawater temperature (T) and salinity (S), to

examine the influence of circulation on subsequent jellyfish distribution, and further, to verify the possible source of jellyfish via ship observations, satellite data, and a particle-tracking experiment. First, the distribution of jellyfish and hydrological characteristics in the YS and ECS were examined based on data from cruises conducted in the latter half of July 2013. Second, satellite data (sea surface temperature; SST, chlorophyll a; Chl-*a*) were used to describe the seasonal variation in water masses from spring to summer. Third, jellyfish and non-jellyfish water masses in July were back-traced to expected source and non-source areas, respectively. Fourth, the particles were released from the source we found to compare with ferry observed jellyfish, and to verify the jellyfish transport. Finally, we evaluated the source and the roles of physical and biological processes in the distribution of giant jellyfish.

3.2. Data and methods

3.2.1. Ship observations

From 14 July 2013 to 1 August 2013, a large-scale survey involving R.V. Dongfanghong II of Ocean University of China, China, and R.V. Nagasakai Maru of Nagasaki University, Japan, was conducted in a cooperative way within the exclusive economic zones of these countries and a portion of the exclusive economic zone of Korea. A total of 74 stations covering the western YS and ECS and 38 covering the eastern ECS just south of Jeju were covered by the R.V. Dongfanghong II and the R.V. Nagasaki Maru, respectively. There were some cross-stations just south of Jeju affected by the CDW. T and S were measured by conductivity-temperature-depth (CTD) profilers (Sea-Bird Electronics, Inc., SBE911 plus) on the two ships, and 5 m depth data were used for this study.

The ferry observations of giant jellyfish were conducted from young medusa stage visible to eye in early June until October, 2013 between Shimonoseki (Osaka), Japan and Qingdao (Shanghai), China. All the ferry observations in YS from early June and late July (June 8-9, June 23-25, July 7-9 and July 21-23), which were generally coincided with our particle tracking experiments and field observation, were selected for our comparison. The details of the jellyfish observation by ferry were same as in the two scientific cruises, as will be described in section 2.2.

3.2.2. Visual observation of giant jellyfish

Visual counts of giant jellyfish were conducted during the daytime from the upper deck of the vessels, except during experiments and meal times. The giant jellyfish could be distinguished easily because of the color difference between seawater and their reddish-brown bodies (Yoon et al., 2008). The observation distance from the ship and time interval of counting were 10 m and 5 min, respectively. Jellyfish number, location [latitude and longitude], and time were recorded between each time interval. Jellyfish abundance was calculated based on these counts and the area covered during each observation track.

3.2.3. Satellite data

MODIS AQUA Nighttime Level 3 daily and monthly SST products from before and during the cruise (April–August) were obtained from Physical Oceanography Distributed Active Archive Center (http://podaac.jpl.nasa.gov). We used the high quality SST products as described by Xu et al. (2013). GOCI Level-2 daily data from April through July, 2013 were obtained from the Korea Ocean Satellite Center (KOSC) (http://kosc.kordi.re.kr/). These daily data were binned monthly, resulting in Chl-*a*

product. These daily data were binned monthly, resulting in Chl-*a* product. All SST and Chl-*a* data processing was conducted using NASA SeaDAS software (version 6.4) and Windows Image Manager (WIM) software (http://www.wimsoft.com/).

3.2.4. Japanese 25-year Reanalysis data

Wind data from Japanese 25-year Reanalysis (JRA-25) with 1.125° × 1.125° spatial resolution were obtained from the Japan Meteorological Agency (JMA) (*Onogi et al*., 2007) (http://jra.kishou.go.jp/JRA-25/index_en.html).

3.2.5. Statistics and cluster analysis

The kriging interpolation technique was used to obtain a high spatial resolution ($0.05^{o}\times0.05^{o}$) Temperature (T) and salinity (S) value among field stations. The jellyfish track station in each time interval (5 minutes) was resampled in a 3×3 window in the interpolated field datasets to retrieve T-S parameters. The field survey and jellyfish track stations were resampled in a 3×3 window in the model T-S datasets to obtain corresponding T-S data.

For clustering analysis of water mass characteristics, T and S were normalized by the standard deviation independently, and then used to determine water mass cluster according to the Euclidean distance between each sample. The grouping method was hierarchical clustering, which has been widely used in analyzing water masses in the YS and ECS (Quan et al., 2013). The basic principle of the hierarchical clustering method is described by *Chen et al.,* (2011).

3.2.6. Flow filed and Lagrangian particle tracking experiment

Flow fields of the Japan Coastal Ocean Predictability Experiment 2 (JCOPE2) (Miyazawa et al., 2009) model output results during spring to summer 2013 were used

for the back-tracing of water masses with and without the jellyfish. The model was developed based on the Princeton Ocean Model with a generalized coordinate of sigma (Mellor et al., 2002) and provides daily mean ocean current data covering the western North Pacific (10.5–62°N, 108–180°E) with a horizontal resolution of 1/12° and 46 vertical levels. The model is driven by wind stresses and heat and salt fluxes. The combination of a state-of-the-art eddy-resolving ocean general circulation model and remote and in situ observational data produce realistic high-resolution data. The JCOPE2 data well reproduced the mean water mass properties of in situ observations in the western North Pacific (Miyazawa et al., 2009).

We used a backward-in-time trajectory (BITT) model, without the random-walk process, to find the potential source area of the giant jellyfish (Isobe et al., 2009). The forward-in-time trajectory (FIIT) model were also conducted to verify the backward trajectory as suggested by Batchelder (2006) and Isobe et al. (2009), considering the diffusion influence. The particle locations $[\mathbf{X}=(x,y)]$ at time $t-\Delta t$ and $t+\Delta t$ were calculated in a backward and forward way, respectively (Batchelder, 2006; Isobe et al., 2009):

$$\mathbf{X}^{t-\Delta t} = \mathbf{X}^{t} - \mathbf{U}\Delta t - \frac{1}{2}\left(\mathbf{U}\cdot\nabla_H \mathbf{U} + \frac{\partial \mathbf{U}}{\partial t} \right)\Delta t^2$$

and

$$\mathbf{X}^{t+\Delta t} = \mathbf{X}^{t} + \mathbf{U}\Delta t + \frac{1}{2}\left(\mathbf{U}\cdot\nabla_H \mathbf{U} + \frac{\partial \mathbf{U}}{\partial t} \right)\Delta t^2 + R\sqrt{2K_h \Delta t(\mathrm{i},\mathrm{j})}\,,$$

where $\mathbf{U}[=(u,v)]$ and K_h are current vectors and diffusivity computed at 3 m depth in JCOPE2, Δt is the time step (0.05 day), R is a random number generated at each time step with an average and standard deviation of 0.0 and 1.0, respectively. **i** and **j** are

unit vectors in the x and y directions, respectively. The particle simulation is halted when the particles hit the land.

The jellyfish were considered particles transported only by ocean currents, without consideration of biological and ecological features such as swimming or vertical migration. In the backward particle experiments, seven particles representing a high abundance of counted jellyfish (>0.001 ind. m^{-2} in a value of more than 30 min) were released from the jellyfish track stations, respectively (Fig. 3.1, Table 3.1). Particles representing all of the observed jellyfish in each experiment were back-traced until 1 May 2013, when ephyrae were expected to be liberated. In the same way, nine particles representing a water mass without jellyfish (</=0.001 ind. m^{-2} in a value of more than 30 min) were back-traced until 1 May (Fig. 3.1, Table 3.1). The released particles in the water masses with and without jellyfish generally represented all of the areas with high- and low-abundance of jellyfish during the cruises covering the entire areas of the YS and ECS (Fig. 3.1, Table 3.1). In the forward particle tracking experiments, 400 particles were released on May 1 in the source identified by BIIT, with corresponding SST varied 15±2°C. These particles were forward traced until end of July to compare with the ferry observed jellyfish and to verify transport of jellyfish from source.

3.3. Results

3.3.1. Hydrological characteristics and jellyfish distribution

3.3.1.1. Distribution of SST and salinity

SST varied between 21°C and 29°C during the observations, with low-temperature water (<24°C) in the mouth of the Changjiang and higher-temperature water (>25.5°C) toward the southeast in the ECS (Fig. 3.2a). SST was relatively low in the northwest of

the Shandong Peninsula (<24°C), and high (>26°C) at 123°E, 35°N. It was evenly distributed in the offshore regions of the ECS, ranging from 27°C to 29°C. However, it was particularly low (20–21°C) at the mouth of the Changjiang, even compared to the stations in the YS, which indicates that upwelling occurred during the cruise (Fig. 3.2a). The salinity distribution showed significant difference in the YS and ECS (Fig. 3.2b). Relatively high-salinity water (>32), covering the area from offshore of Zhejiang through the region south of Taiwan, was dominant in the southern ECS (Fig. 3.2b). The CDW, characterized by low salinity (<30), dominated the northern ECS, spread northeastward to the southern YS, and then turned southeastward until reaching the Okinawa Trough (Fig. 3.2b). An obvious salinity front (30.5–31) extended southeastward from the mouth of the Changjiang to the region west of Okinawa (Fig. 3.2b).

3.3.1.2. Water masses in the surface layer

Based on the T-S properties measured during the cruises, eight main water masses were identified by the cluster analysis: CDW, South Yellow Sea Water (SYSW), North Yellow Sea Water (NYSW), Taiwan Warm Current (TWC), Kuroshio Warm Current (KWC), Changjiang Mouth Upwelling Water (CUW), CDW-TWC mixed water, and CDW-KWC mixed water (Fig. 3.3), which have been identified and studied previously (Ichikawa and Beardsley 2002; Lv et al. 2006; Yuan et al. 2008). The CDW, characterized by low salinity (<31) and a wide temperature range (25–29°C), covered a large area from the mouth of the Changjiang eastward and southeastward to the region south of Jeju (Figs. 3.3 and 3.4). Based on relatively small changes in temperature (22°C to 27°C) and salinity (29.5 to 31.5), the SYSW was located at the northern

stations. The TWC and KWC dominated the offshore regions of the ECS, except for the coastal areas of Zhejiang and Shanghai, and temperature and salinity were highest in these regions, varying from 26°C to 29°C and from 32 to 34, respectively. The CUW was clearly observed at the mouth of the Changjiang, where temperature was low (26–29°C) and salinity was high (32–33), compared to the surrounding CDW(Figs. 3.3 and 3.4). Mixed waters of different water masses were also identified during the cruises (Figs. 3.3 and 3.4). Only two stations were located in CDW-TWC mixed water, but more stations were in CDW-KWC mixed water in the region south of Jeju. The temperature and salinity of these two water masses have similar characteristics, as some studies have regarded the TWC as a branch of the KWC (Yuan et al., 2008). Waters with low temperature (20–21°C) and medium salinity (30.5–31) observed at three stations in the northern YS were different from those in the southern YS.

3.3.1.3. Spatial distributions of the jellyfish during the cruise

The spatial distribution of the jellyfish in the YS and ECS showed significant heterogeneity. Jellyfish abundance showed a general decreasing gradient from Chinese coastal areas to the open sea, according to the observations from the two ships (Fig. 3.4). A high abundance of jellyfish (0.05–0.10 ind. m^{-2}) was continuously observed along the Qingdao coast. High abundances of jellyfish were also found in the middle of the YS, north of the mouth of the Changjiang, and west of Jeju Island, with abundances varying from 0.01 to 0.05 ind. m^{-2} (Fig. 3.4). Jellyfish abundance was relatively low at the northwestern edge of the Shandong Peninsula and south of the mouth of the Changjiang, where it varied from 0.0001 to 0.001 ind. m^{-2}. Few jellyfish were observed in the Changjiang offshore region, south of Jeju, and in the southern ECS (Fig. 3.4). Few jellyfish were also observed in the Jiangsu offshore area and at the eastern boundary of

the YS, where high abundance has been reported previously (Zhang et al., 2012). Most of the locations with abundant jellyfish were located in the SYSW or in mixed waters such as the CDW-KWC and CDW-CUW. Small numbers of jellyfish (0.0001–0.001 ind. m^{-2}) were found in the NYSW and in the CUW-TWC mixed water (Fig. 3.4).

3.3.2. Seasonal variation of water mass and wind in YS and ECS coast

The 15 ^{o}C isotherm in April was formed along the continental shelf (100 m isobath) of ECS, extending from Zhejiang offshore toward Jeju Island. Most of the YS and northern ECS was dominated by the cold surface water (< 15 ^{o}C) (Fig. 3.5a). The cold water (< 15 ^{o}C) extended from YS coast toward south or southeast until the middle of northern ECS. Chl-*a* was high (> 1.5 mg m^{-3}) from coast of YS toward the southwest of Jeju (Fig. 3.5c). This southeastward extension of high Chl-*a* plume corresponded with 50 m isobaths (Figs. 3.1, 3.5c), indicating the mixing of the shallow waters largely contributed to the high Chl-*a* concentration. High Chl-*a* (> 1.5 mg m^{-3}) was also observe in the middle of YS, indicating the spring bloom probably occurred with the seasonal warming (Xu et al., 2013). In May, the 15 ^{o}C isotherm distributed from the northern Jiangsu coast toward Changjiang mouth, and then extended east until southwest of Jeju island. The water was relatively warmer at the Jiangsu coast than offshore of YS; this warming pattern was highlighted by a northward intruding tongue from along Jiangsu coast (Fig. 3.5d). The high Chl-*a* (> 1.5 mg m^{-3}) region shrank within the 50 m isobaths (Fig. 3.5f). High Chl-*a* plume in northern Jiangsu coast corresponded to the 20 m isobaths, this Chl-*a* plume in Jiangsu offshore was found not connected with the high Chl-*a* in Changjiang offshore, compare to that in April (Figs. 3.1, 3.5f). In June, SST became warmer than 15 ^{o}C with the seasonal warming in the YS and ECS. SST was homogeneous in the Jiangsu coast, northeastward offshore and its

adjacent middle of YS, characterized by warm water (21-22 ^{o}C) at the west of colder upwelled water with temperature ranging from 17 to 18 ^{o}C (Fig. 3.5g). High Chl-a region (> 1.5 mg m^{-3}) was found to shrink within 20 m isobath (Figs. 3.1, 3.5i). The offshore region was depleted, characterized by low Chl-a, with the intensifying stratification. In July, seasonal warming reached its maximum, SST in Jiangsu coast and Changjiang mouth inlet was significantly warmer (> 28 ^{o}C). The similar water with lower temperature (around 26 ^{o}C) was observed in its northeastward offshore and middle of YS (Fig. 3.5j). The distribution pattern of SST in the Jiangsu coast and its northeastward offshore was similar as that in June. Meanwhile, Chl-*a* was increasing from coast toward offshore, the high Chl-a region (> 1.5 mg m^{-3}) expanded until southwest of Jeju, showing similar pattern but with higher Chl-a concentration in coast as that in April (Fig. 3.5l). The coast runoffs contributed significantly of the enhancement of phytoplankton obviously, as July was characterized by the rainy season.

In April, the wind generally blew from north in this month, and it was weak (< 1 m s^{-1}) in the YS and ECS coast, compared to the offshore (Fig. 3.5b). In May, the wind blew strongly from south along the Chinese coast in the YS (> 3 m s^{-1}) (Fig. 3.5e). In June, the wind blew west toward the coast of YS from the east, with the same magnitude as in May (Fig. 3.5h). In July, the wind blew toward north, and becoming much stronger (> 4 m s^{-1}), compared to previous months (Fig. 3.5k).

3.3.3. Particle Tracking Experiments

3.3.3.1. Transport of jellyfish-the particle simulation

To find the possible source of the jellyfish and verify the advection of water masses from their origins, seven particles with jellyfish (J1, J2,…J7) and nine particles

without jellyfish (N1, N2,…N9) were traced from the observation date until 1 May 2013 (Fig. 3.1, Table 1).

In July, the simulated trajectory results generally corresponded with the distribution of satellite SST. Most of the particles with jellyfish (J2, J3, J4, and J7) and several particles without jellyfish (N1, N2, N9) in the YS were traced westward to the middle of the YS, as a result of the influence of the dominant strong eastward current (Fig. 3.6a and b). Only one particle with jellyfish (J1) was traced back to the region south of Qingdao. The particles with jellyfish near the mouth of the Changjiang and its offshore region (J5, J6) were back-traced to the mouth of the Changjiang and to Hangzhou Bay, respectively, while the particles without jellyfish were back-traced to the mouth of the Changjiang (N3, N6) and to Hangzhou Bay (N4, N7, N8) in early July, except for particle N5, which returned to the Zhejiang offshore region (Fig. 3.6a and b). It is noted that the backward trajectories of J2, J3, J4, and J7 show good agreement with the distribution of west–east warm water (25–26°C) in the middle of the YS. The trajectories of the particles (J3, J4) in the south, even with shorter tracing time, were longer than those in the north (J1, J2, J7, N1, N2, and N9) (Fig. 3.6a and b).

In June, the pathways of J2, J3, J4, and J7 were showing a northeastward trajectory; these particles were traced back to southern Jiangsu offshore (J4) and northern Jiangsu offshore waters (J2, J3, J7, and N1) in early June (Fig. 3.6c and d). Particles N2 and N9 were traced back with shorter distances to the middle of the YS under the influence of the very weak current (Fig. 3.6c and d). Particles J1, J5, N3, N4, N6, N7, and N8 disappeared as they were traced to areas approaching land to the south of Qingdao (J1) and to the mouth inlet of the Changjiang (J5, N3, N4, N6, N7, and N8). The most southern particle (N5) was traced back to the south Zhejiang nearshore waters

(Fig. 3.6c and d). The satellite SST showed that warm water was distributed from the coast of Jiangsu to its northeast offshore region (Fig. 3.6c). The distribution corresponded well with the trajectories of J2, J3, J4, J7, and N1. The strong easterly and mild southeasterly winds in the Jiangsu offshore and northern YS coast contributed to the northward and northeastward flow, respectively, thus the northward path of J4 was dominant and the northeastward paths of J2, J3, and J7 were main components, compared to July (Fig. 3.6c and d).

Particles J2, J3, J4, J7, N1, N2, N5, and N9 were finally traced back to early May, whereas other particles could not be traced until early May as they progressively reached land. Particles J2, J3, and J7 were traced back to the Jiangsu coast with an SST of nearly 15°C (Fig. 3.6e and f). Particle N1 was also traced back to the coast of Jiangsu. N4 returned to the mouth of the Changjiang, whereas N5 was traced back to the Taiwan Strait, offshore of Fujian Province. Particles N2 and N9 remained in the middle of the YS, as a result of the weak current there. The northward intrusion of the 15°C isotherm agreed well with the north or northeastward paths of particles (J2, J3, J4, J7, and N1) from the coast to offshore (Fig. 3.6e and f). The alongshore wind at the southern YS coast induced a current that flowed north or northeastward (Fig. 3.5d), explaining the trajectories of these particles.

3.3.3.2. Comparisons of observed and modeled water masses

To assess the differences between the model and field data, we compared the modeled and observed results of T-S properties (Figs. 3.7 and 3.8). The modeled and ship-observed T-S diagrams generally corresponded with each other, especially for the

water masses SYSW, TWC, and KWC. However, other water masses such as CDW, CUW, and NYSW showed significant differences. Significant overestimation of the influence of the Changjiang River led to salinities as low as 20 at stations near the river mouth (Figs. 3.7 and 3.8). In addition, the stations in the SYSW, especially the west station near Haizhou Bay, were nearest to the NYSW in the model T-S diagram but far from the NYSW in the field T-S diagram (Fig 3.8). These results indicate that the station nearest the NYSW in the model was influenced heavily by the NYSW. This was further confirmed by the modeled temperature intrusion of cold water to the north Jiangsu coast, where it was not shown by the field temperature (Fig. 3.7a).

3.3.3.3. Verification of transport of jellyfish: Forward Particle Simulation

Transport of jellyfish from the identified source was verified by the forward tracking experiments. Generally, the forward trajectories of most particles were consistent with warm water distribution (Fig. 3.6a, c and e) and the backward trajectories of particles (J2, J3, J4, J7, N2 and N9) (Fig. 3.6b, d and f) in the YS from May to July. The distributions of the forward particles were also compared with the jellyfish distribution by ferry observation. In June, most of the particles were still near the northeastern Jiangsu offshore, not transported to the middle of YS. Meanwhile, the jellyfish were not observed in the middle of YS in early and late June according to the ferry observation. The ferry results supported the distributions of these particles in June. These particles were transported to the middle of YS in early July, gradually extending southeastward until north of Jeju in the late July (Fig. 3.9). The high abundance of jellyfish were also observed by ferry in the middle of YS in early July, and widely distributed in the YS until the area near Jeju in the late July. These distributions of

particles corresponded well with distribution of ferry observed jellyfish in early and late July, respectively.

3.4. Discussion

3.4.1. Jellyfish Distribution and Relation with Water Mass

Our results of high abundance in the SYSW and the CDW-CUW and CDW-KWC mixed waters and low numbers in the CDW-TWC mixed water, KWC, and CDW suggest that jellyfish were concentrated mostly in the YS and northern ECS, with a salinity range of 30.5–31 (Figs. 3.3 and 3.4), and hardly observed in the southern ECS. This finding is consistent with previous large-scale studies, such as that of Zhang et al. (2012), who found that the giant jellyfish was confined to the water masses of the YS and northern ECS, mostly concentrated in the salinity range of 32–33, and that few were observed in the water masses of the southern ECS. The slight salinity difference between our study and that of Zhang et al. (2012) was probably caused by the difference of observation method: net survey in Zhang et al. (2012) and visual counting in present study, which reflects differences in sampling depth. In addition, the interannual differences in river runoff and its interactions with KWC intrusion will also introduce difference. Yoon et al. (2008), using visual observations, reported a high abundance of jellyfish to the west of Jeju and few to the east and south of Jeju. This further supports our findings of a high abundance in the YS and northern ECS and a low abundance in the southern ECS, and suggests that the circulation in the YS and northern ECS played an important role in the spatial distribution and transport of jellyfish from spring to summer. The transport of jellyfish in the YS is discussed in the next section.

3.4.2. Seasonal Variation in Water Masses and Its Relationship with Jellyfish Transport in the YS and ECS

Jellyfish distribution and transport were highly associated with the circulation and variation in water masses described in section 4.1. We found that the north or northeastward flow during May to July was an important factor for the spatial distribution in the YS and northern ECS and that CDW, with its intensified northeastward plume from May to July, was another factor that blocked the jellyfish from moving into the southern ECS. The finding of north or northeastward flow at the YS coast is generally consistent with studies of green algae (Lee et al., 2011; Huo et al., 2013), which originate from the Jiangsu coast (Liu et al., 2009; Hu et al., 2010). The slight difference in drift pattern was probably caused by differences in the responses of algae and jellyfish to wind, where the algae show a quick response because they generally float at the surface whereas jellyfish remain in the water column (Qiao et al., 2011). This difference would result in the relatively nearshore distribution of green algae and offshore distribution of jellyfish in the YS, considering the north and northwestward winds from May to July, which was confirmed by our observations during these cruises.

The results of the jellyfish particle trajectories in the YS, which reflected the modeled flow pattern, indicate that the jellyfish particles were transported northward, northward or northeastward, and eastward in May, June, and July, respectively. The wind blows northwestward, westward or northwestward, and northward, in May, June, and July, respectively. If we considered the surface current induced by wind always turn clockwise with the angle around 0-90° to the wind direction, the wind was highly correlated with the jellyfish particle trajectories in the YS in May, June and July, respectively. In addition, our satellite SST data indicated that cold water (<15°C) extended southeastward to the middle of the northern ECS in April and that warm water

(>15°C) intruded north or northeastward to the offshore region of the YS from May to July (Fig. 3.5a and c). The jellyfish trajectories obtained from the particle-tracking experiments corresponded well with the distribution of warm water (Fig. 3.6), suggesting that ephyrae advection probably started in late April to early May when ephyrae were liberated from polyps in the source region, the Jiangsu coast. The mild southerly (transitional) wind in April (Fig. 3.5b), which is unfavorable for northward flow, further supports young jellyfish advection beginning in late April to early May. The origins of the jellyfish will be discussed in the next section. Our finding of the wind force responsible for the north or northward flow is consistent with those of previous studies (Liu et al., 2009; Lee et al., 2011; Qiao et al., 2011; Wang et al., 2013; Huo et al., 2013). All of these studies confirmed the presence of a north or northward distribution of water from the coast of Jiangsu in spring and summer. This northward flow driven by southerly wind, in combination with Jiangsu coastal west–east radial tidal sand ridges (Huo et al., 2013), as well as the CDW, would block the southward movement of water masses, thus trapping jellyfish during May to July. These water masses would be more easily transported northward to the southern YS and its offshore areas from May to July, as confirmed by our particle-tracking experiments.

3.4.3. Jellyfish Source

The main source location of giant jellyfish polyps in the YS and ECS has not yet been found (Toyokawa et al., 2012; Kawahara et al., 2013). Our study based on young medusae available for visual observation coupled with satellite data and a particle-tracking experiment provided a reasonable estimate of the source area. Laboratory experiments have suggested that the source should be characterized by a critical temperature for strobilation and growth of ephyrae, a suitable substrate for

polyps, and enough food for ephyrae survival (Uye 2008, 2011; Purcell et al., 2012; Kawahara et al., 2013). Majority of the jellyfish particles in the YS (J2, J3, J4 and J7) were back-traced to the Jiangsu coast, when the temperature was nearly 15°C in early May (Fig. 3.6e). The similar T-S properties of these particles between the model and field data indicate that the water masses with a high abundance of jellyfish were good indicators for tracing the source (Fig. 3.7 and 3.8). In laboratory experiments, ephyrae are liberated from polyps after a rise in water temperature from 13°C to 23°C (Kawahara et al., 2006), and a recent study found that a temperature of 15°C induces the highest cumulative strobilation rate (Kawahara et al., 2013). The back-traced particles in early May coincided with a temperature change from below 15°C to higher temperatures in the northern Changjiang region and Jiangsu coast. This indicates that the Jiangsu coast is a highly possible source.

Nevertheless, the particles observed near Qingdao (J1) and the Changjiang offshore region (J5 and J6) returned to the south coast of Qingdao and the Changjiang mouth and Changjiang mouth inlet regions, respectively (Fig. 3.6a). The T-S properties of J5 and J6 were significantly different between the model and field data (Figs 3.7 and 3.8) because they were influenced by low-salinity water in the model. This suggests the possible overestimation of CDW in this area in the model. The model error in this area made estimation unattainable. The water mass properties at the Qingdao coast could not be studied because of an absence of field data. However, the south coast of Qingdao was probably not a source because the temperature in early July was too high (>21°C), resulting in a very low strobilation rate (Kawahara et al., 2013).

Furthermore, the particles without jellyfish were scattered in the YS and ECS, as described in section 3.3.3 (Fig. 3.6b, d and f). The particles observed in the western

(N2) and northern (N9) areas were always traced to the middle of the YS, an area characterized by low temperature (<12°C) and deep water (>50 m) near the YS trough in early May (Fig. 3.6f). The low temperature for strobilation and the fine-grained bottom sediment (Yuan et al., 2008), which is not suitable polyp substrate (Uye, 2008; Kawahara et al., 2013), provide support for denying the middle of the YS as a source. The N5 particle observed to the south of Jeju returned to the southern ECS near the Taiwan Strait, where the temperature was always too high (>23°C) from May to July. The area of the Taiwan Strait is influenced significantly by the KWC, which is characterized by temperatures too high for strobilation. Also, neither ephyrae nor giant jellyfish have ever been found in this southern area. Thus, it is reasonable to reject the southern ECS near the Taiwan Strait as a source.

Particle N1 was a special case that was traced to the Jiangsu coast, which is hypothesized to be a source (Fig. 3.6e and f). The T-S properties of N1 between the model and field data indicated that it was nearest to the northernmost water mass, NYSW, in the model and thus easily influenced by the southward extension of cold water from the NYSW, as described in section 3.3.3.2. However, the satellite data did not show the cold water intrusion (Fig. 3.6a). The model error probably resulted in the water mass without jellyfish being back-traced to the Jiangsu coast, which we expect to be the most likely source area. The T-S properties of all of the particles in the water mass without jellyfish near the mouth of the Changjiang (N3, N4, N6, N7, and N8) were different between the model and field data as they were influenced significantly in the model by CDW, as described for J5 and J6 (Figs. 3.7 and 3.8). The model error led us to estimate the paths with high uncertainty. However, there remains a possibility that the Changjiang mouth region is also a source (Moon et al., 2010), because jellyfish are

abundant in mixed water including CDW. Studies need to focus on update the numerical model results with more accuracy in future.

Considering hydrological, biological, and ecological factors, these results show that the coast of Jiangsu is a highly possible source of the jellyfish. The Jiangsu coast was also confirmed as the source of green algae, which have traditionally been distributed widely and intensively in the YS, especially in the summer of 2008 (Hu et al., 2010; Huo et al., 2013). This source area is known for heavy aquaculture of seaweed and for using bamboo as substrate for cultured seaweed, which may provide a new good substrate for jellyfish polyps to attach to in the shallow coastal waters. We found that the high abundance of jellyfish at the Qingdao coast coincided with large patches of green algae. The transport of the green algae from the coast of Jiangsu provides further support that the Jiangsu coast is the source of the jellyfish, although the drift patterns may be slightly different. The jellyfish transport from the source we found were verified by releasing particles in the Jiangsu coast on May 1, and forward traced until end of July. It is undoubtedly that the trajectories of particles corresponded well with backward trajectories of jellyfish particles in YS, because both the experiments followed the same flow field, though there is slightly difference influenced by the diffusion term (Fig. 3.9). The ferry observed jellyfish from its appearance until the widespread distribution showed good agreement with the distributions of jellyfish particles (Fig. 3.9). The consistency between independent ferry observation and forward traced particles further support that jellyfish were transported from Jiangsu coast to the northeast offshore from May to July in the YS. Food availability should be important for the survival of ephyrae, and a previous satellite study indicated that the coastal areas always have high Chl-*a* concentration and that a match between the ephyra stage and phytoplankton blooms

always occurs on the Jiangsu coast (Xu et al., 2013). This would provide good food conditions for ephyrae survival if the high Chl-*a* corresponds with high zooplankton which is the jellyfish prey. However, whether and how the food availability influences ephyrae, or even adult jellyfish, needs to be studied further in the future.

3.5. Conclusions

High abundances of giant jellyfish were observed in the SYSW and in CDW-CUW and KWC-CDW mixed waters, whereas few jellyfish were observed in other water masses. This indicates that the circulations in the YS and ECS play an important role in the spatial distribution during spring to summer. Variation in satellite SST was used to characterize seasonal variation in the water masses, and the results indicated that as the winter monsoon weakened and seasonal heating strengthened, a water mass with warmer SST (>15°C) at the Jiangsu coast in May was extending northward and northeastward until July. The southerly wind was probably an important factor determining this northeastward transport. This indicates that the wind contributed to the advection of young medusae from the coast to the northward offshore regions starting in the end of April to early May. Water masses with jellyfish traced back to the northern Jiangsu coast in May. In addition, water masses without jellyfish were traced back to the mouth of the Changjiang River, and the Taiwan Strait. These findings indicate that the high abundance of giant jellyfish observed in the YS and ECS in July came from the Jiangsu coast in May when ephyrae were probably liberated from polyps there as SST increased from below 15°C to higher values. The trajectories of water masses with jellyfish from May to July obtained by particle-tracking experiments were consistent with the distribution of warm water, indicating that the coast of Jiangsu is a highly possible source of the jellyfish.

Table 3.1 Water mass with and without jellyfish represented by the particles in the particle tracking experiments

Particle No.	longitude	latitude	Water mass	With or without jellyfish	Observed date
J 1	120.65	35.95	SYSW	jellyfish	2013-7-14
J 2	121.78	35.00	SYSW	jellyfish	2013-7-16
J 3	123.96	34.45	SYSW	jellyfish	2013-7-18
J 4	124.79	33.65	SYSW	jellyfish	2013-7-24
J 5	123.30	32.00	CDW	jellyfish	2013-7-25
J 6	122.98	31.97	CDW	jellyfish	2013-7-31
J 7	123.00	35.02	SYSW	jellyfish	2013-8-1
N 1	121.36	35.00	SYSW	No jellyfish	2013-7-16
N 2	123.50	35.00	SYSW	No jellyfish	2013-7-18
N 3	122.60	33.20	SYSW	No jellyfish	2013-7-19
N 4	122.80	31.00	CDW	No jellyfish	2013-7-20
N 5	125.74	31.01	TWC-CDW	No jellyfish	2013-7-21
N 6	125.85	31.87	CDW-KWC	No jellyfish	2013-7-23
N 7	123.03	31.65	CDW	No jellyfish	2013-7-25
N 8	123.00	31.04	CDW-TWC	No jellyfish	2013-7-31
N 9	123.09	35.53	SYSW	No jellyfish	2013-8-1

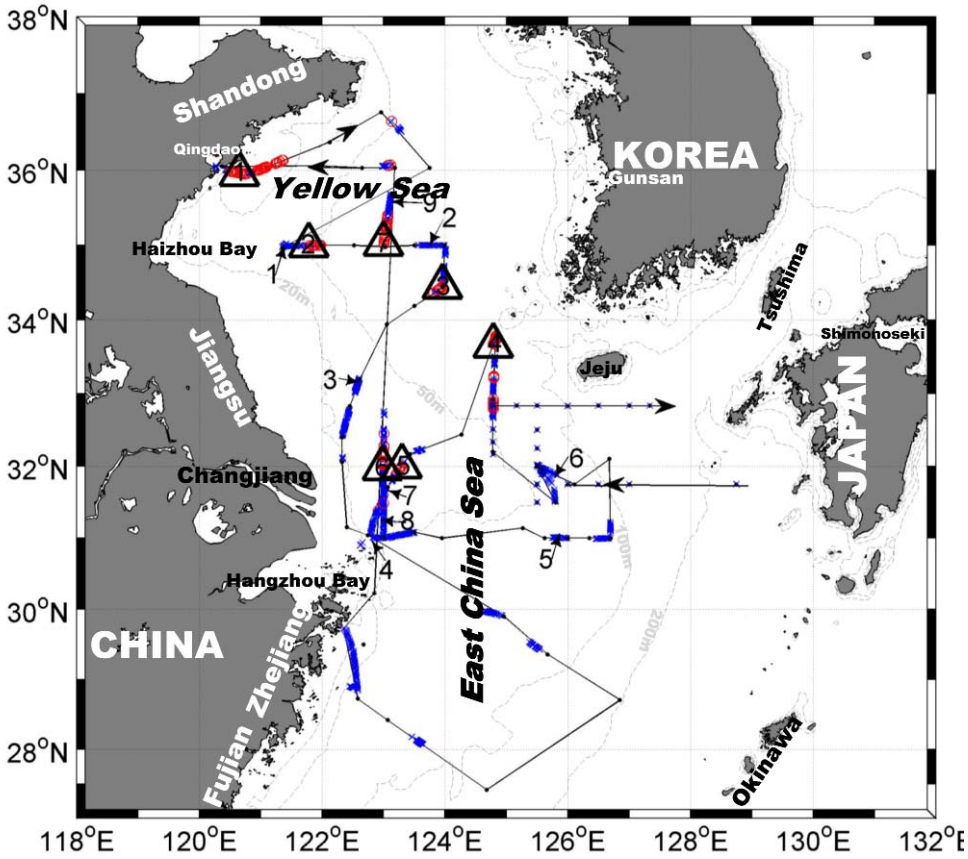

Fig. 3.1. Ship route (black line) and departure and arrival directions (big arrows). The red circles and blue crosses indicate high (>0.001 ind. m^{-2}) and low (<=0.001 ind. m^{-2}) abundances of jellyfish, respectively. The numbers with and without a triangle represent water masses with (>0.001 ind. m^{-2}) and without (<=0.001 ind. m^{-2}) jellyfish, respectively. The 50, 100, and 200 m isobaths are indicated by the dash gray lines. The labels with white capital, white small letters indicate the names of countries, provinces/cities, respectively. Black italic and black normal letters indicate the names of seas, islands, bays, and river, respectively.

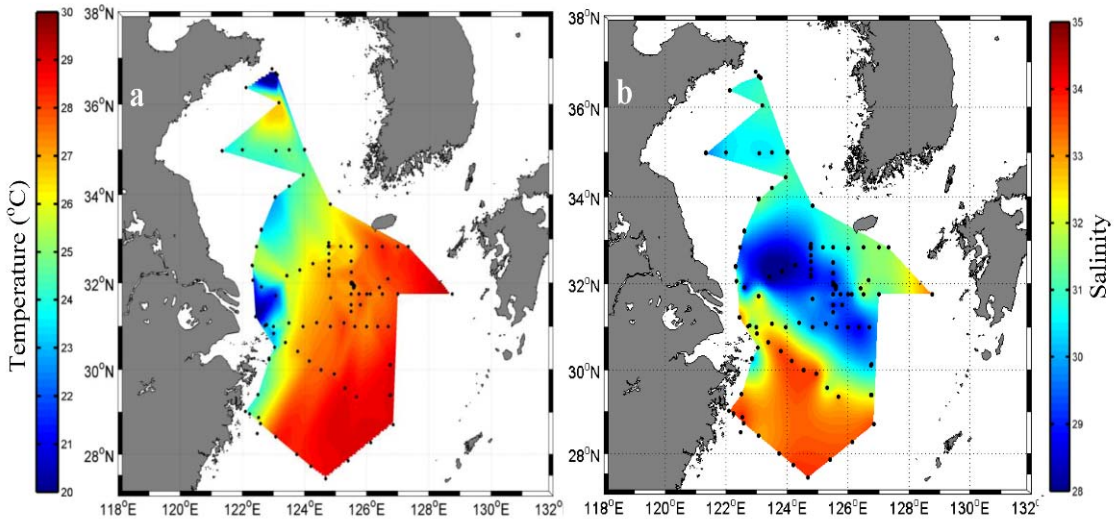

Fig. 3.2 Distributions of surface temperature (a) and salinity (b) during the cruises. Black dots indicate CTD stations.

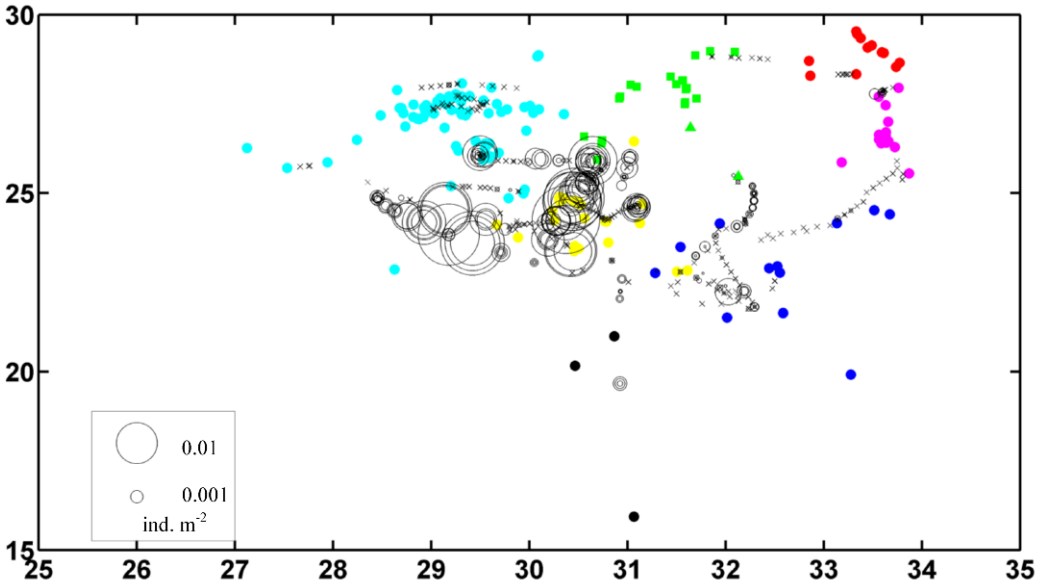

Fig. 3.3 T-S diagrams (5 m) overlain with jellyfish abundance. Dots colors indicate water masses according to T-S properties. Red, pink, yellow, black, cyan and blue dots indicate KWC, TWC, SYSW, NYSW, CDW and CUW respectively; green triangles denote CDW-TWC and green squares denote CDW-KWC; (see text for the abbreviations). Temperature and salinity data on jellyfish tracks without CTD stations were interpolated by the Kriging technique, as described in section 3.2.5. Black circles indicate jellyfish abundance (ind. m^{-2}). Black crosses indicate areas without jellyfish.

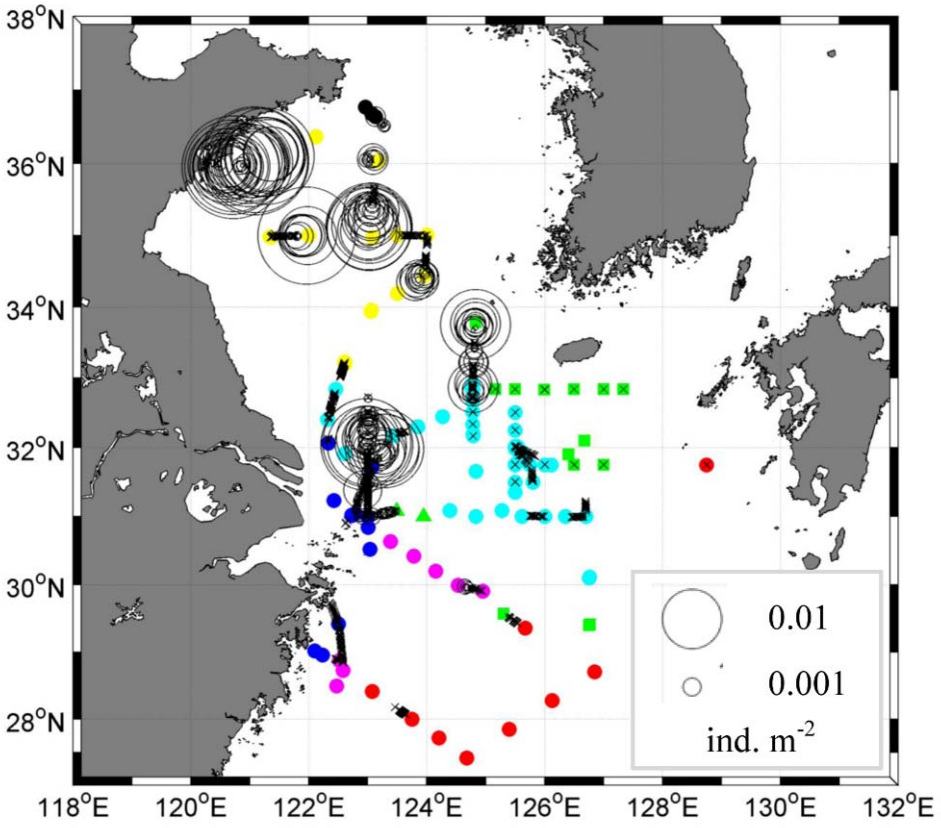

Fig. 3.4 Geographical distributions of water masses overlain with jellyfish abundances. The colors and symbols are the same as in Figure 3.3

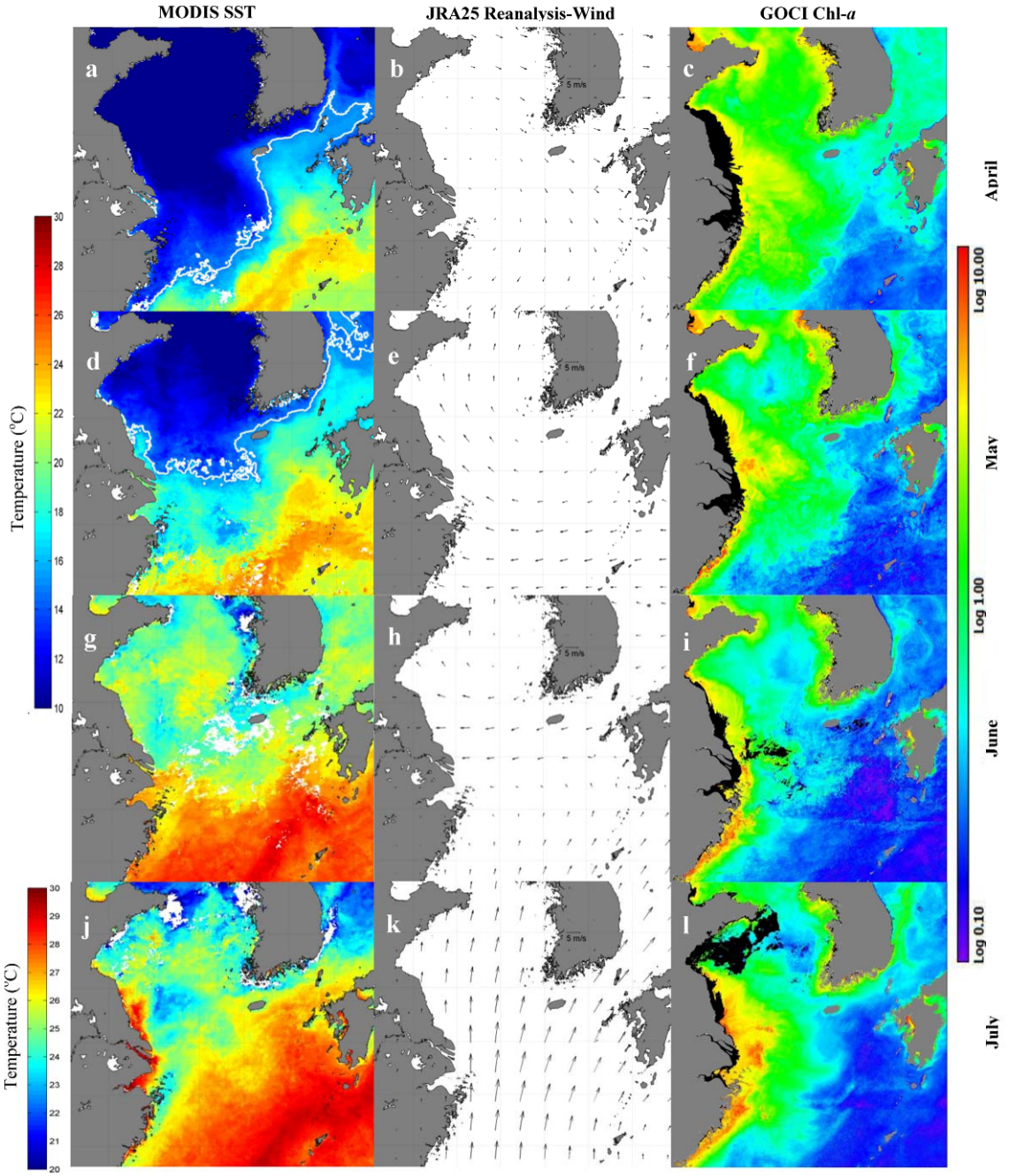

Fig. 3.5 Distributions of MODIS satellite SST (a, d, g, j), JRA25 reanalysis wind (b, e, h, k) and GOCI Chl-*a* (c, f, i, l) in April (a, b, c), May (d, e, f), June (g, h, i) and July (j, k, l), 2013, respectively. The white lines in Apirl (a) and May (c) MODIS SST images indicated 15 ^{o}C isotherms. The black pixels indicated not valid data.

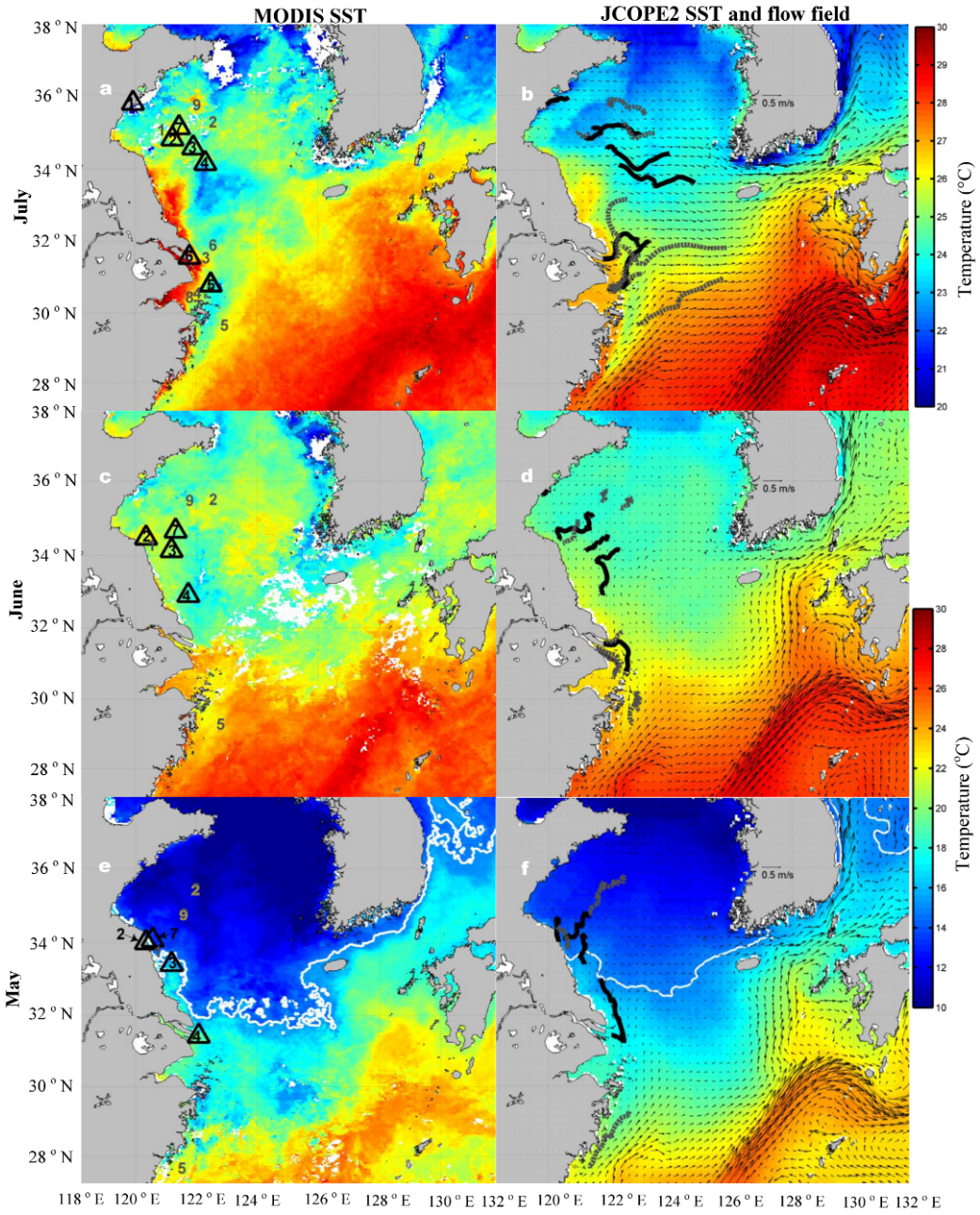

Fig. 3.6 MODIS monthly mean SST (a, c, e) and JCOPE2 monthly mean SST/flow fields (b, d, f) from July to May 2013, respectively, overlain with backward particle-tracking experiments of water masses with and without jellyfish. Black solid and dark gray dotted lines indicate backward trajectories of water masses with and without jellyfish, respectively, during the month. The numbers with and without triangles indicate the final traced position (until the first day) of the month of each particle during the month in the experiment. The numbers with and without triangles indicate water masses with and without jellyfish, respectively. The white line in May (e, f) indicates the 15°C isotherm.

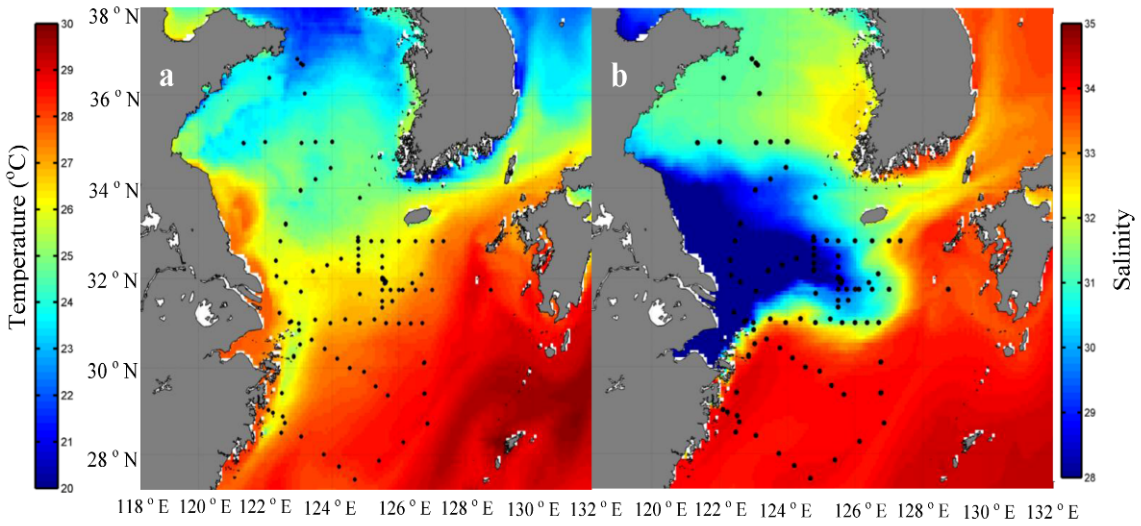

Fig. 3.7 Distributions of SST (a) and salinity (b) retrieved from JCOPE2 at the corresponding days and locations (dots) during the cruises.

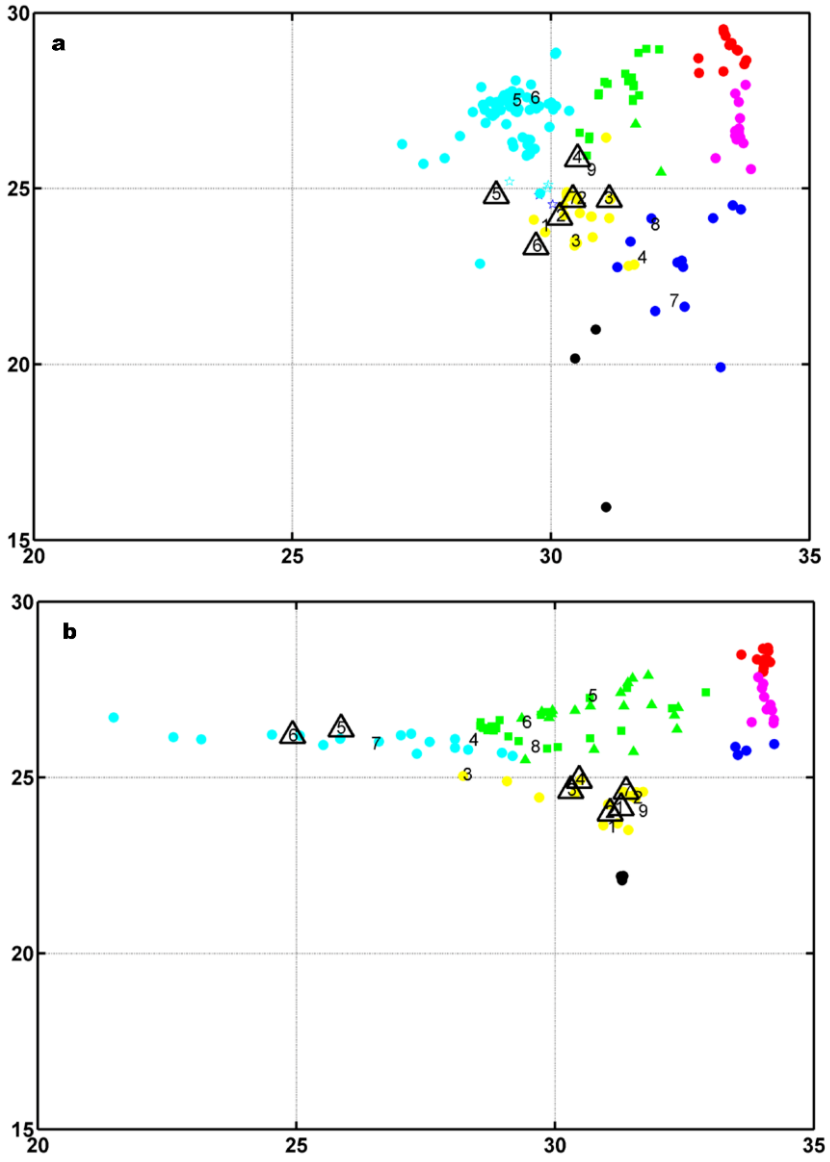

Fig. 3.8 Ship observed (a) and modeled (b) T-S diagrams overlain by the start positions of the backward particle trajectories. The different colors indicate various water masses as in Figure 3.3. The numbers with and without triangles indicate water masses with and without jellyfish, respectively, traced by the backward particle-tracking experiments (same as in Fig. 3.1).

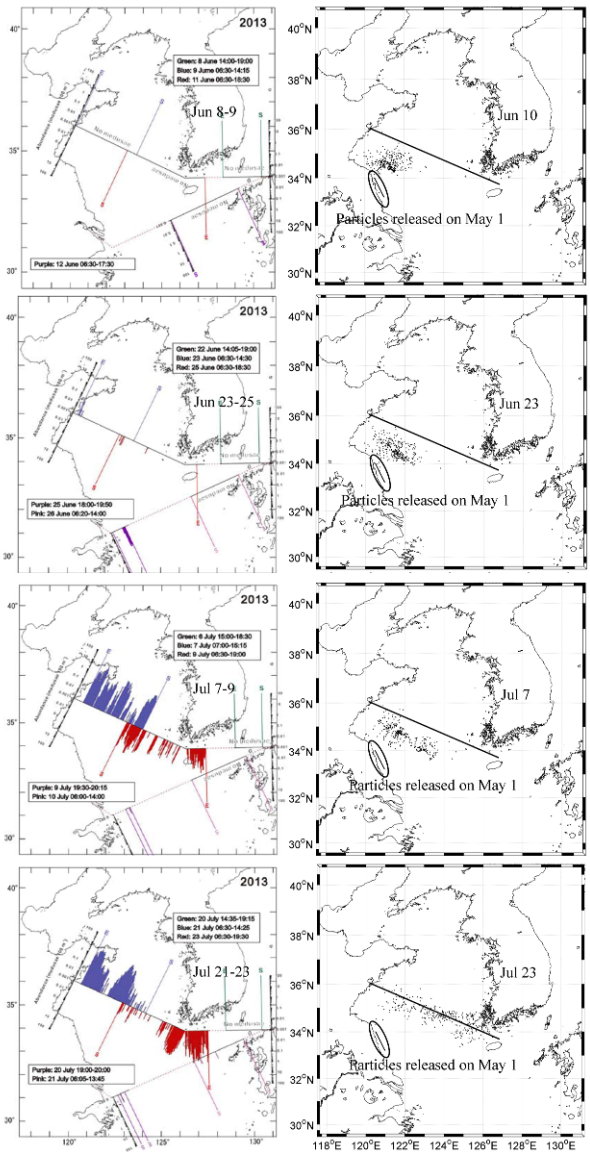

Fig. 3.9. Distributions of ferry observed jellyfish (left panel) and particles trajectories by FIIT (right panel) from June to July. Different colors indicate the observation in different days, as also shown inside the box. Lines S and E indicate the start and end of the observation, respectively. Jellyfish abundance along the ferry lines were calculated same way as described in section 2.2, except the unit as ind. $100m^{-2}$. The scale bar of abundance was also shown vertically to the ferry lines in the left panels. Distributions in early June, late June, early July and late July were shown from the top to bottom panels, respectively. The black lines in the right panel indicate ferry lines in the YS, as conducted by the left panels. Particles released in the Jiangsu coast on May 1 were shown in the elongated circles.

Chapter 4: General Discussion

In chapter 2, we studied the jellyfish outbreaks by three hypotheses revealed by satellite SST and Chl-*a*. To our knowledge, no work had yet done to study jellyfish outbreaks by satellite data. We found that warm temperature and high eutrophication level could make a jellyfish outbreak through the affect on the survival of ephyrae.

In chapter 3, Jellyfish transport from the potential source was studied by satellite data, coupling with trajectory model. Few studies were done about jellyfish transport from potential source in a combination study. Moon et al. (2010) found that the Changjiang mouth is a possible source according to the forward trajectory model. However, Moon did not consider the temperature influecen on the polyp strobilation and ephyral stage, which is very important for the source verification. Our combination study confirmed the source in the north Changjiang mouth through Jiangsu coast, considering the temperature influence on polyp strobilation and ephyrae stage in the YS and ECS.

In Chapter 4, we will discuss the environments for polyp and ephyral stage in the sources we found in Chapter 3. The three hypotheses will also be checked according to recent couple of years in the sources.

SST was significantly increasing from 1985 to 2007 ($r > 0.5$, $p < 0.05$), and it was significantly decreasing from 1998 to 2013 ($r < -0.5$, $p < 0.05$) during spring to summer in both two areas (Figs. 4.2 and 4.3). The low temperature in 2008, 2010 and 2011 lead the significant decreasing trend of recent 15 years. The maximum SST was attained in PJY and JY indicated the warmer temperature was necessary condition for the jellyfish outbreaks. Significant lower temperature in 2008, 2010 and 2011 corresponded with non-outbreak years. Low temperature in 2008, 2010 and 2011 was a determined factor

to make a non-outbreak year. SST in 2012 and 2013 was relatively lower in March and April, similar as that of NJY, but increasing significantly to higher temperature in middle May to June, similar as that of JY (Figs. 4.2 and 4.3). This made the tsst15 in 2012 and 2013 between those of JY and NJY. The medium abundance of jellyfish (between outbreak and absence) observed in 2012 and 2013 corresponded with middle tsst15. Temperature hypothesis was consistent with that in Chapter 2 in source areas.

Chl-*a* were increasing significantly during spring to summer from 1998 to 2013 in both two areas (Fig. 4.4). The high eutrophic condition did not corresponded to the medium jellyfish outbreaks in 2012 and 2013, indicating eutrophication was necessary, but not sufficient condition for the medium outbreak in 2012 and 2013. However, less eutrophic condition was probably a limited factor for jellyfish outbreak. Eutrophication hypothesis was consistent with that in Chapter 2 in source areas.

It is undoubted that match between phytoplankton bloom and ephyral stage was always found in the source region of CSYS and CJE, because these regions were coastal areas of Chapter 2. The match/mismatch condition also cannot explain the medium jellyfish outbreak in the two years.

Match/mismatch hypothesis was consistent with that in Chapter 2 in source areas.

The middle temperature, especially the medium timing of 15^{o}C, was probably a determined factor to decide the medium jellyfish abundance. This indicates the magnitude of jellyfish outbreak was probably quantitatively related with timing of 15^{o}C in the source region. However, whether they are linearly or non-linearly correlated need further investigation.

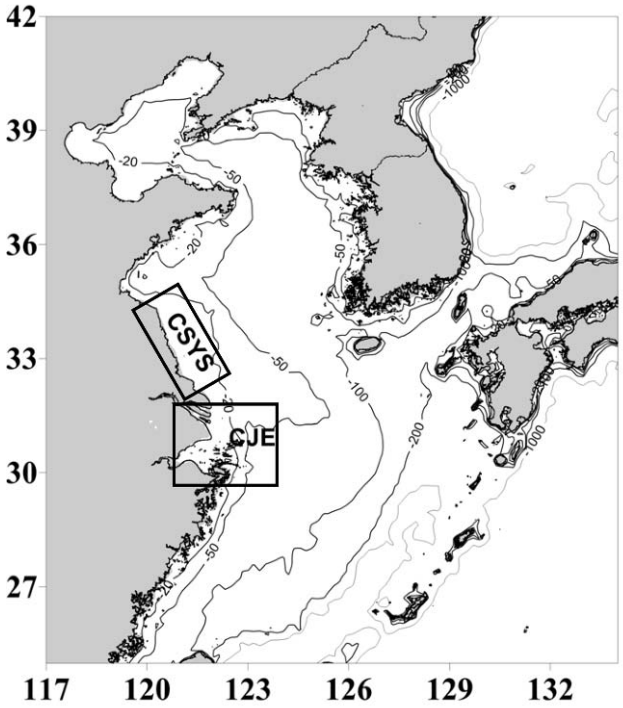

Fig. 4.1 Investigated source areas according to trajectory model

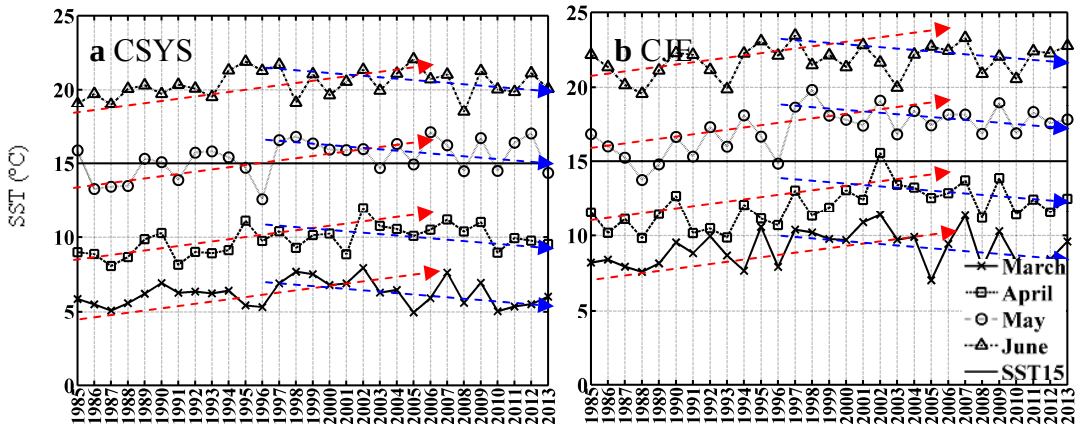

Fig. 4.2 Interannual variability in monthly SST during spring to summer (March-June) from 1985 to 2013 in the source areas **a** *CSYS* and **b** *CJE*. Red and blue arrows indicate significant increasing ($r > 0.5$, $p < 0.05$) and decreasing trend ($r < -0.5$, $p < 0.05$)

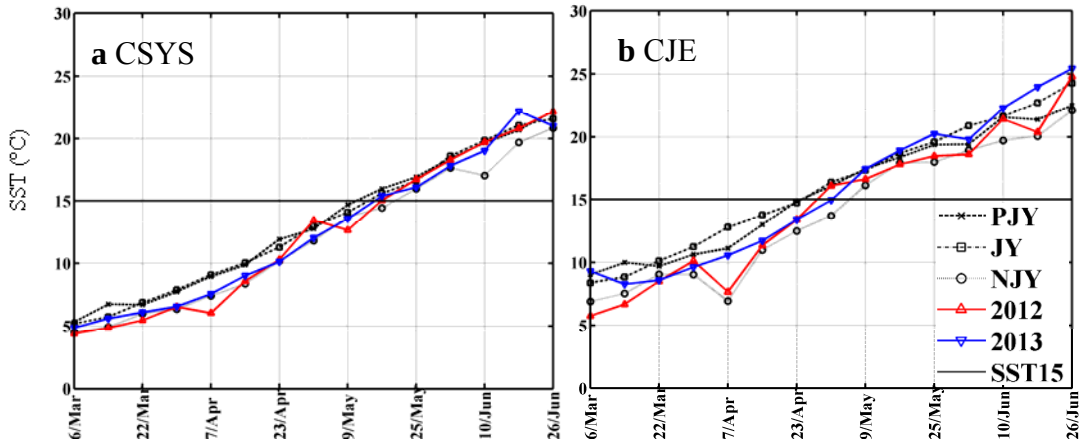

Fig. 4.3 Seasonal variation in SST of PJY, JY, NJY, 2012 and 2013 during spring to summer in the source areas **a** *CSYS* and **b** *CJE*.

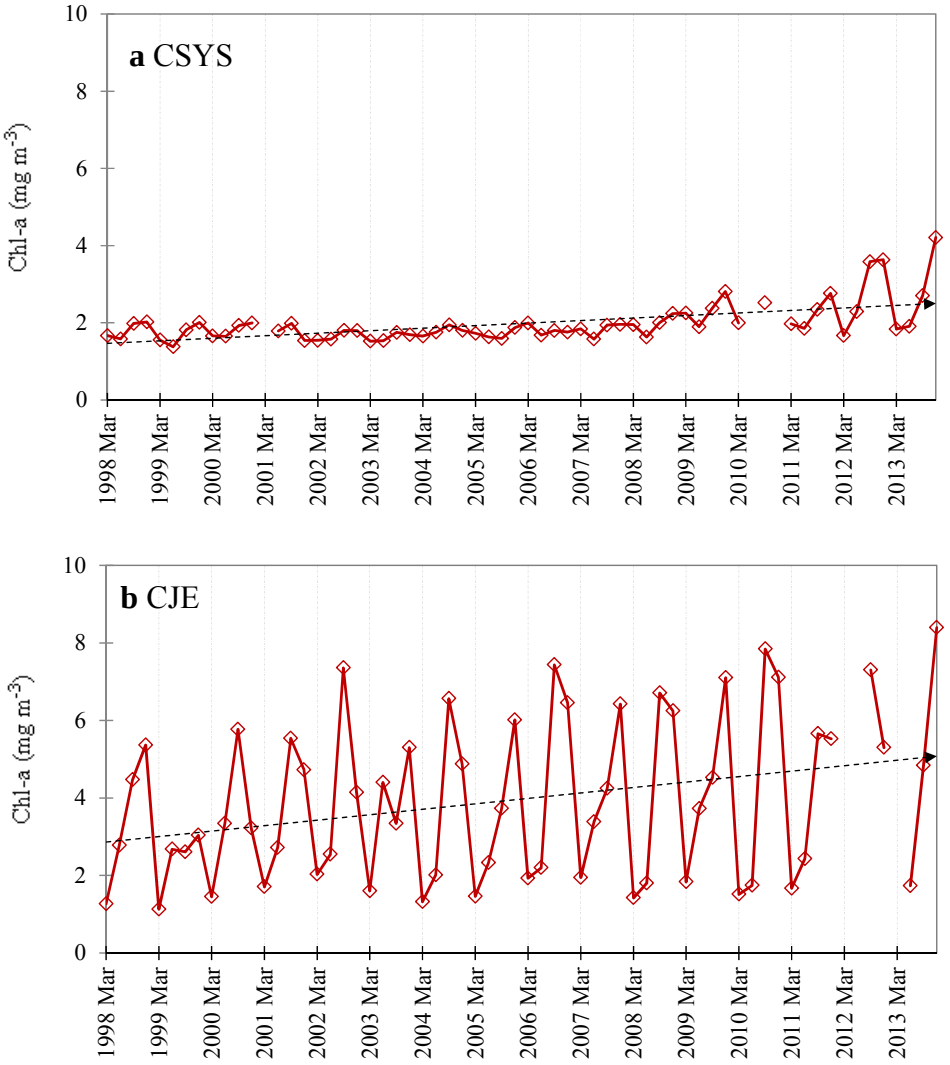

Fig. 4.4 Interannual variability in monthly Chl-*a* during spring to summer (March-June) from 1998 to 2013 in the source areas **a** *CSYS* and **b** *CJE*. Black dash arrows indicate significant increasing trend

Chapter 5: General Conclusion

5.1. Concluding Remarks

Interannual variation of abundance and seasonal transport of *N. nomurai* were studied by satellite data, in combination with ship observation and particle tracking model.

The warming of seawater, in combination with increased eutrophic conditions in late spring and early summer were necessary conditions for the increase in *N. nomurai* outbreaks in JY. However, significantly lower SST was a determined factor to prevent the outbreaks of *N. nomurai* in NJY, probably through effects on survival of ephyra. Match/mismatch to phytoplankton bloom could not explain the interannual variation of jellyfish outbreaks or its absence.

We found that the high abundances of giant jellyfish were in southern YS water, mixed waters including CDW, while few were observed in southern ECS water, the transport of giant jellyfish from source by circulation in the YS and ECS were confirmed by ship observation, satellite data, coupling with trajectory model. The water mass with jellyfish traced back to the northern Jiangsu coast in May when SST was nearly 15^{o}C. Additionally, water mass without jellyfish were traced back to Changjiang mouth and Taiwan Strait. These findings indicated that the high abundance of giant jellyfish observed in YS in July came from Jiangsu coast in late April or early May when the SST was near 15 ^{o}C (indicator of polyp strobilation or ephyral stage). Wind probably contributed to the transport of jellyfish northward or northeastward from May to July.

Finally, a conceptual model was developed using satellite SST and Chl-*a*, enabling the prediction of jellyfish outbreak in advance easily. Furthermore, the study also

proposed an important method to find the source and to verify transport of giant jellyfish using ship observation, satellite data, and trajectory model. This method provided a better and reasonable way to estimate the source from the early appearance of young jellyfish, which was visible to human eye.

5.2. Future Research Directions

Due to seasonally high abundance of giant jellyfish and their extremely high consumption rates on copepods (Uye 2011), jellyfish significantly impact zooplankton via predation. As the main prey of *N. nomurai* medusae are small copepods and gastropod larvae (with size <1 mm) that may directly feed on phytoplankton (Uye 2008), the jellyfish abundance was positively correlated with small and medium size zooplankton (Yoon et al., 2008). Thus, the changes in zooplankton populations and its community structure, especially copepods, have the potential to affect jellyfish abundance via bottom-up process (positive relation). Moreover, jellyfish also influence the zooplankton through top-down process (negative relation). How these two processes function in the marine ecosystem was still unknown. It is necessary to know the zooplankton's role in jellyfish outbreak. In addition, as zooplankton have the potential to alter the ecosystem through both bottom-up and top-down processes, it is also necessary to know role of zooplankton in "phytoplankton-zooplankton-jellyfish" food web, and the implication of this food web for jellyfish outbreak.

Prediction of giant jellyfish outbreaks is very important to prevent the damage of fisheries activities. Our study suggested satellite SST in spring can be a good indicator of jellyfish abundance in summer. Jellyfish abundance was obtained by ferry boats in the YS and ECS during 2006 through 2013 (Uye personal communication). The environments in spring, especially SST, are expected to be highly correlated with

average abundance during these years; this enables the estimation of jellyfish abundance in forthcoming summer available with the SST in spring. Thus, it is necessary to study the relation between summer jellyfish abundance and spring satellite SST in the potential source, and to predict the jellyfish outbreaks or absence in the near future.

References

Ahn YH and Shanmugam P (2006) Detecting the red tide algal blooms from satellite ocean color observations in optically complex Northeast-Asia Coastal waters. Remote Sens Environ 103(4):419-437. doi: 10.1016/j.rse.2006.04.007

Båmstedt U, Wild B and Martinussen M (2001) Significance of food type for growth of ephyrae *Aurelia aurita* (Scyphozoa). Mar Biol 139(4):641-650. doi: 10.1007/s002270100623

Beardsley RC, Limeburner R, Yu H, and Cannon GA (1985) Discharge of the Changjiang (Yangtze River) into the East China Sea. Cont Shelf Res 4(1-2): 57-76

Chai CZ, Yu M, Song XX and Cao XH (2006) The Status and Characteristics of Eutrophication in the Yangtze River (Changjiang) Estuary and the Adjacent East China Sea, China. Hydrobiologia 563(1):313-328. doi: 10.1007/s10750-006-0021-7

Cushing DH (1990) Plankton production and year-class strength in fish populations: an update of the match/mismatch hypothesis. Adv Mar Biol 26:249-294. doi: 10.1016/S0065-2881(08)60202-3

Dong, Z. J., D. Y. Liu, and J. K. Keesing (2010), Jellyfish blooms in China: Dominant species, causes and consequences, Mar. Poll. Bull., *60*(7), 954-963.

Durant JM, Hjermann DO, Anker-Nilssen T, Beaugrand G, Mysterud A, Pettorelli N, and Stenseth NC (2005) Timing and abundance as key mechanisms affecting trophic interactions in variable environments. Ecology Letters 8:952–958. doi: 10.1111/j.1461-0248.2005.00798.x

Frank KT, Petrie B and Shackell NL (2007) The ups and downs of trophic control in continental shelf ecosystems. Trends Ecol Evol 22(5):236–242. doi:10.1016/j.tree.2007.03.002

Fuchs, B., Wang W., Graspeuntner S., Li Y. Z., Insua S., Herbst E. M., Dirksen P., Bohm A. M., Hemmrich G., Sommer F., Domazet-Loso T., Klostermeier U. C., Anton-Erxleben F., Rosenstiel P., Bosch T. C. G. and Khalturin K. (2014) Regulation of Polyp-to-Jellyfish Transition in Aurelia aurita. Curr Biol, 24 (3), 263-273.

Furuya K, Hayashi M and Yabushita Y (2003) Phytoplankton dynamics in the East China Sea in spring and summer as revealed by HPLC-derived pigment signatures. Deep Sea Res Part II 50:367-387. doi: 10.1016/S0967-0645(02)00460-5

Gao C and Zhang T (2010) Eutrophication in a Chinese Context: Understanding Various Physical and Socio-Economic Aspects. AMBIO 39(5-6):385-393. doi: 10.1007/s13280-010-0040-5

Gao XL and Song JM (2005) Phytoplankton distributions and their relationship with the environment in the Changjiang Estuary, China. Mar Pollut Bull 50(3):327-335. doi: 10.1016/j.marpolbul.2004.11.004

Gremillet D, Lewis S, Drapeau L, van Der Lingen CD, Huggett JA, Coetzee JC, Verheye HM, Daunt F, Wanless S and Ryan PG (2008) Spatial match-mismatch in the Benguela upwelling zone: should we expect chlorophyll and sea-surface temperature to predict marine predator distributions? J Appl Ecol 45(2):610-621. doi: 10.1111/j.1365-2664.2007.01447.x

Henson SA and Thomas AC (2007) Interannual variability in timing of bloom initiation in the California Current System. J Geophys Res 112(C08007):1-12. doi: 10.1029/2006JC003960

Hickox (2000) Climatology and seasonal variability of ocean fronts in the East China, Yellow and Bohai seas from satellite SST data. Geophys Res Lett (27):2945–2948. doi: 10.1029/1999GL011223

Honda, N., T. Watanabe, and Y. Matsushita (2009), Swimming depths of the giant jellyfish *Nemopilema nomurai* investigated using pop-up archival transmitting tags and ultrasonic pingers, *Fish. Sci*, *75*(4), 947-956.

Hu C, Li D, Chen CS, Ge JZ, Muller-Karger FE, Liu JP, Yu F and He MX (2010) On the recurrent Ulva prolifera blooms in the Yellow Sea and East China Sea. J Geophys Res 115:C05017. doi: 10.1029/2009JC005561.

Huo, Y. Z., J. H. Zhang, L. P. Chen, M. Hu, K. F. Yu, Q. F. Chen, Q. He, and P. M. He (2013), Green algae blooms caused by *Ulva prolifera* in the southern Yellow Sea: Identification of the original bloom location and evaluation of biological processes occurring during the early northward floating period, *Limnol. Oceanogr.*, *58*(6), 2206-2218.

Ichikawa, H., and R. C. Beardsley (2002), The current system in the Yellow and East China Seas, *J. Oceanogr.* , *58*(1), 77-92.

Jiao N, Zhang Y and Zeng Y (2007) Ecological anomalies in the East China Sea: Impacts of the Three Gorges Dam? Water Res 41(41):1287-1293. doi: 10.1016/j.watres.2006.11.053

Kang YS, Jung S, Zuenko Y, Choi I, Dolganova N (2012) Regional differences in the response of mesozooplankton to oceanographic regime shifts in the northeast asian marginal seas, Prog Oceanogr, 97:120-134. doi: 10.1016/j.pocean.2011.11.012

Kaufman L and Rousseeuw PJ (1990) Finding Groups In Data: An Introduction to Cluster Analysis, John Wiley & Sons, p 368

Kawahara MS, Uye S, Ohtsu K and Izumi H (2006) Unusual population explosion of the giant jellyfish *Nemopilemia nomurai (Scyphozoa : Rhizostomeae)* in East Asian waters. Mar Ecol Prog Ser 307:161-173. doi:10.3354/meps307161

Kawahara M, Ohtsu K and Uye S (2013) Bloom or non-bloom in the giant jellyfish *Nemopilema nomurai* (Schphozoa: Rhizostomeae): roles of dormant podocysts. J Plankton Res 35(1):213-217. doi:10.1093/plankt/fbs074.

Kim, D., Sang Hwa Choi, Kyung Hee Kim, JeongHee Shim, Sinjae Yoo, and C. H. Kim (2009), Spatial and temporal variations in nutrient and chlorophyll-*a* concentrations in the northern East China Sea surrounding Cheju Island, *Cont. Shelf Res.*, *29*(11-12), 1426-1436.

Kim HC, Yamaguchi H, Yoo S, Zhu JR, Okamura K, Kiyomoto YK, Tanaka K, Kim SW, Park T, O IS and Ishizaka J (2009) Distribution of Changjiang Diluted Water Detected by Satellite Chlorophyll-a and Its Interannual Variation during 1998–2007. J Oceanogr 65:129-135. doi: 10.1007/s10872-009-0013-0.

Kiorboe T and Nielsen TG (1994) Regulation of Zooplankton Biomass and Production in a Temperate, Coastal Ecosystem1. Copepods. Limnol Oceanogr 39(3):493-507.

Lee HE, Yoon WD and Lim D (2008) Description of feeding apparatus and mechanism in *nemopilema nomurai* kishinouye (scyphozoa: rhizostomeae). Ocean Sci J 43(1):61-65. doi: 10.1007/BF03022432

Lee, J. H., I. C. Pang, I. J. Moon, and J. H. Ryu (2011), On physical factors that controlled the massive green tide occurrence along the southern coast of the Shandong Peninsula in 2008: A numerical study using a particle-tracking experiment, *J. Geophys. Res.*, 116(C12), doi: 10.1029/2011JC007512.

Li MT, Xu K, Watanabe M and Chen Z (2007) Long-term variations in dissolved silicate, nitrogen, and phosphorus flux from the Yangtze River into the East China Sea and impacts on estuarine ecosystem. Estuar Coast Shelf S 71(1-2):3-12. doi: 10.1016/j.ecss.2006.08.013.

Lin C, Ning X, Su J, Lin Y and Xu B (2005) Environmental changes and the responses of the ecosystem of the Yellow Sea during 1976–2000. J Mar Sys 55(3-4):223-234. doi: 10.1016/j.jmarsys.2004.08.001.

Liu, D. Y., J. K. Keesing, Q. U. Xing, and P. Shi (2009), World's largest macroalgal bloom caused by expansion of seaweed aquaculture in China, *Mar. Poll. Bull.*,

58(6), 888-895.

Lv, X. G., F. L. Qiao, C. S. Xia, J. R. Zhu, and Y. L. Yuan (2006), Upwelling off Yangtze River estuary in summer, *J. Geophys. Res.*, 111(C11), doi: 10.1029/2005JC003250.

Lynam CP, Hay SJ and Brierley AS (2004) Interannual variability in abundance of North Sea jellyfish and links to the North Atlantic Oscillation. Limnol Oceanogr 49(3):637-643. doi: 10.4319/lo.2004.49.3.0637

Lynam CP, Hay SJ and Brierley AS (2005) Jellyfish abundance and climatic variation: contrasting responses in oceanographically distinct regions of the North Sea, and possible implications for fisheries. J Mar Bio Assoc UK 85:435-450. doi: 10.1017/S0025315405011380.

Mellor, G. L., S. Hakkinen, T.Ezer, and R. Patchen (2002), A generalization of a sigma coordinate ocean model and an intercomparison of model vertical grids, in *In Ocean Forecasting: Conceptual Basis and Applications*, edited by N. Pinardi and J. D. Woods, pp. 55-72, Springer, New York.

Michael PF and Proschan MA (2010) Wilcoxon-Mann-Whitney or t-test? On assumptions for hypothesis tests and multiple interpretations of decision rules. Statistics Surveys 4:1-39. doi: 10.1214/09-SS051

Minnett PJ, Evans RH, Kearns EJ and Brown OB (2002) Sea-surface temperature measured by the Moderate Resolution Imaging Spectroradiometer (MODIS). IEEE International Geosciences and Remote Sensing Symposium. Toronto, Canada.

Miyazawa, Y., R. C. Zhang, X. Y. Guo, H. Tamura, D. Ambe, J. S. Lee, A. Okuno, H. Yoshinari, T. Setou, and K. Komatsu (2009), Water Mass Variability in the Western North Pacific Detected in a 15-Year Eddy Resolving Ocean Reanalysis, *J. Oceanogr.* , *65*(6), 737-756.

Moon, J. H., N. Hirose, and J. H. Yoon (2009), Comparison of wind and tidal contributions to seasonal circulation of the Yellow Sea, *J. Geophys. Res.*, 114(C8), doi: 10.1029/2009JC005314

Moon, J. H., I. C. Pang, J. Y. Yang, and W. D. Yoon (2010), Behavior of the giant jellyfish *Nemopilema nomurai* in the East China Sea and East/Japan Sea during the summer of 2005: A numerical model approach using a particle-tracking experiment, *J. Mar. Sys.* , *80*(1-2), 101-114.

Onogi, K., J. Tslttsui, H. Koide, M. Sakamoto, S. Kobayashi, H. Hatsushika, T. Matsumoto, N. Yamazaki, H. Kaalhori, K. Takahashi, S. Kadokura, K. Wada, K. Kato, R. Oyama, T. Ose, N. Mannoji, and R. Taira (2007), The JRA-25 reanalysis, *J Meteorol Soc Jpn*, *85*(3), 369-432.

Platt T, Sathyendranath S and Fuentes-Yaco C (2007) Biological oceanography and fisheries management: perspective after 10 years. ICES J Mar Sci 64:863-869. doi: 10.1093/icesjms/fsm072

Purcell JE, Uye S and Lo WT (2007) Anthropogenic causes of jellyfish blooms and their direct consequences for humans: a review. Mar Ecol Prog Ser 350:153–174. doi: 10.3354/meps07093

Purcell JE, Hoover RA and Schwarck NT (2009) Interannual variation of strobilation by the scyphozoan *Aurelia labiata* in relation to polyp density, temperature, salinity, and light conditions in situ. Mar Ecol Prog Ser 375:139-149. doi: 10.3354/meps07785

Purcell JE (2012) Jellyfish and Ctenophore Blooms Coincide with Human Proliferations and Environmental Perturbations. Annu Rev Marine Sci 4:209-235. doi: 10.1146/annurev-marine-120709-142751.

Qiao, F. L., G. S. Wang, X. G. Lu, and D. J. Dai (2011), Drift characteristics of green macroalgae in the Yellow Sea in 2008 and 2010, *Chin. Sci. Bull.*, *56*(21), 2236-2242.

Quan, Q., X. Y. Mao, X. D. Yang, Y. Y. Hu, H. Y. Zhang, and W. S. Jiang (2013), Seasonal variations of several main water masses in the southern Yellow Sea and East China Sea in 2011, *J. Ocean Univ. China*, *12*(4), 524-536.

Richardson AJ, Andrew B, Hays GC and Gibbons MJ (2009) The jellyfish joyride: causes, consequences and management responses to a more gelatinous future. Trends Ecol Evol 24(6):312-322. doi: 10.1016/j.tree.2009.01.010

Siswanto E, Nakata H, Matsuoka Y, Tanaka K, Kiyomoto Y, Okamura K, Zhu JR and Ishizaka J (2008) The long-term freshening and nutrient increases in summer surface water in the northern East China Sea in relation to Changjiang discharge variation. J Geophys Res 113:C10030. doi: 10.1029/2008JC004812

Siswanto E, Tang J and Yamaguchi H, Ahn YH, Ishizaka J, Yoo S, Kim SW, Kiyomoto Y, Yamada K, Chiang C and Kawamura H (2011) Empirical ocean-color

algorithms to retrieve chlorophyll-a, total suspended matter, and colored dissolved organic matter absorption coefficient in the Yellow and East China Seas. J Oceanogr 67(5):627-650. doi: 10.1007/s10872-011-0062-z

Sommer U and Lengfellner K (2008) Climate change and the timing, magnitude, and composition of the phytoplankton spring bloom. Global Change Biol 14(6):1199-1208. doi: 10.1111/j.1365-2486.2008.01571.x

Tang DL, Di BP, Wei GF, Ni IH, Oh IS and Wang SF (2006) Spatial, seasonal and species variations of harmful algal blooms in the South Yellow Sea and East China Sea. Hydrobiologia 568(1):245-253. doi: 10.1007/s10750-006-0108-1

Toyokawa M, Shibata M, Cheng JH, Li HY, Ling JZ, Lin N, Liu ZL, Zhang Y, Shimizu M, Akiyama H (2012) First record of wild ephyrae of the giant jellyfish *Nemopilema nomurai*. Fisheries Sci 78(6):1213-1218. doi: 10.1007/s12562-012-0550-0

Uye S (2008) Blooms of the giant jellyfish *Nemopilema nomurai*: a threat to the fisheries sustainability of the East Asian Marginal Seas. Plankton and Benthos Research 3(Suppl):125–131

Uye S (2011) Human forcing of the copepod-fish-jellyfish triangular trophic relationship. Hydrobiologia 666(1):71-83. doi: 10.1007/s10750-010-0208-9

Vantrepotte V and Melin F (2009) Temporal variability of 10-year global SeaWiFS time-series of phytoplankton chlorophyll a concentration. ICES J Mar Sci (66):1547-1556. doi: 10.1093/icesjms/fsp107

Wang B (2006) Cultural eutrophication in the Changjiang (Yangtze River) plume: History and perspective. Estuar Coast Shelf S (69):471-477. doi: 10.1016/j.ecss.2006.05.010.

Wang, B., Y. Li, and D. L. Yuan (2013), Effects of topography on the sub-tidal circulation in the southwestern Huanghai Sea (Yellow Sea) in summer, *Acta Oceanologica Sinica*, *32*(3), 1-9.

Wang JJ, Tang DL, and Su Y (2010) Winter phytoplankton bloom induced by subsurface upwelling and mixed layer entrainment southwest of Luzon Strait. J Mar Sys 83(3-4):141-149. doi: 10.1016/j.jmarsys.2010.05.006.

Xu, Y. J., J. Ishizaka, H. Yamaguchi, E. Siswanto, and S. Q. Wang (2013), Relationships of interannual variability in SST and phytoplankton blooms with giant jellyfish (*Nemopilema nomurai*) outbreaks in the Yellow Sea and East China Sea, *J. Oceanogr.* , *69*(5), 511-526.

Yamada K and Ishizaka J (2006) Estimation of interdecadal change of spring bloom timing, in the case of the Japan Sea. Geophys Res Lett 33:L02608. doi: 10.1029/2005GL024792

Yamaguchi H, Kim HC, Son YB, Kim SW, Okamura K, Kiyomoto Y and Ishizaka J (2012) Seasonal and summer interannual variations of SeaWiFS chlorophyll a in the Yellow Sea and East China Sea. Prog Oceanogr 105:22-29. doi: dx.doi.org/10.1016/j.pocean.2012.04.004

Yamaguchi H, Ishizaka J, Siswanto E, Son YB, Yoo S and Kiyomoto Y (2013) Seasonal and spring interannual variations in satellite-observed chlorophyll-a in

the Yellow and East China Seas: new datasets with reduced interference from high concentration of resuspended sediment. Cont Shelf Res 59:1-9. doi:10.1016/j.csr.2013.03.009

Yasuda T (2004) On the unusual occurrence of the giant medusa *Nemopilema nomurai* in Japanese waters. Nippon Suisan Gakkaishi (70):380–386 (in Japanese with English abstract).

Yoon, W. D., J. Y. Yang, M. B. Shim, and H. K. Kang (2008), Physical processes influencing the occurrence of the giant jellyfish *Nemopilema nomurai* (Scyphozoa : Rhizostomeae) around Jeju Island, Korea, *J Plankton Res.*, *30*(3), 251-260.

Yuan, D. L., J. R. Zhu, C. Y. Li, and D. X. Hu (2008), Cross-shelf circulation in the Yellow and East China Seas indicated by MODIS satellite observations, *J. Mar. Sys.*, *70*(1-2), 134-149.

Zervoudaki S, Nielsen TG and Carstensen J (2009) Seasonal succession and composition of the zooplankton community along an eutrophication and salinity gradient exemplified by Danish waters. J Plankton Res 31(12):1475-1492. doi: 10.1093/plankt/fbp084.

Zhang, F., S. Sun, X. S. Jin, and C. L. Li (2012), Associations of large jellyfish distributions with temperature and salinity in the Yellow Sea and East China Sea, *Hydrobiologia*, *690*(1), 81-96.

Zhang J, Liu SM, Ren JL, Wu Y and Zhang GL (2007) Nutrient gradients from the eutrophic Changjiang (Yangtze River) Estuary to the oligotrophic Kuroshio

waters and reevaluation of budgets for the East China Sea Shelf. Prog Oceanogr 74(4):449-478. doi: 10.1016/j.pocean.2007.04.019

Zhai L, Platt T, Tang C, Sathyendranath S and Walls RH (2011) Phytoplankton phenology on the Scotian Shelf. ICES J Mar Sci 68(4):781–791. doi:10.1093/icesjms/fsq175.

Zhou M, Shen Z and Yu R (2008) Responses of a coastal phytoplankton community to increased nutrient input from the Changjiang (Yangtze) River. Cont Shelf Res 28:1483-1489. doi: 10.1016/j.csr.2007.02.009

Acknowledgements

The doctor study will be finished since I moved to this stage, happiness as well as depression were always accompanying with the research. Good days with progress in laboratory experiment, paper writing, and drinking party were never forgotten, gloomy days with decreasing spirit of study, anxiousness of waiting papers were also inscribed in my memory.

Whatever happy and sad days, My supervisor, Prof. Joji Ishizaka always encourages and inspires me, not only for the passion of study, being a scientist, but also for the way of communication, sharing and respecting with others. I greatly appreciate Professor Joji Ishizaka's comments, advice and support during these years.

I would like to express my cordial thanks to Prof. Uye Shin-ichi for providing the valuable ferry data and for providing chance to learn much knowledge about jellyfish ecology and biology.

I am grateful to Assc. Prof. Akihiko Morimoto and Prof. Kazuhisa Tsuboki for providing the numerical model code, lighting me of physical oceanography, air-sea interactions and corrections and suggestions on the dissertation.

I would like to appreciate Prof. Zhao Meixun of Ocean University of China and Prof. Zhang Jing of University of Toyama for providing the valuable chance to join the Chinese cruise in the Yellow Sea and East China and sharing the Chinese cruise data.

I would like to thank Prof. Takeshi Matsuno of Kyushu University for providing Nagasaki-maru's data and lighting me of physical oceanography.

I appreciate Assis. Prof. Yoshihisa Mino and Dr. Chiho Skigara to give me helpful comments and suggestions to improve my studies, to make my Japanese life happy and colorful.

Special thanks go to laboratory secretariat Watanabe Ayako, thanks very much for her kindness to being very patient to solve many detail problems for foreign students.

Special thanks also go to Ishizaka laboratory friends Eko Siswanto, Yamaguchi Hisashi, Sarat C. Tripathy, Takuya Okumura, Hayashi Masataka, Wang Shengqiang, Zhu Yuanli, Maure Eligio De Raus, Xu qian, and Morimoto laboratory friends Masashi Ito for their discussions, support and suggestions especially during the study, cruise and laboratory experiments.

I would like to thant the Ministry of Education, Culture, Sports, Science and Technology, Japan (MEXT) for providing me scholarship during the three years study period, and HyARC of Nagoya University employing me half a year.

Finally, I cannot express myself in words, to thank my wife. She was always with me, providing delicious home-made food without any complaint. She always supports my study and was my foundation forever. I am also grateful to my parents and relatives in China for their love and moral support throughout this research period in Japan.